THE INFLUENCE OF RETURN BENDS ON THE DOWNSTREAM PRESSURE DROP AND CONDENSATION HEAT TRANSFER IN TUBES

Donald P. Traviss
Warren M. Rohsenow

Report No. DSR 72591-75

American Society of Heating, Refrigeration, and Air Conditioning Engineers
Contract No. ASHRAE RP63

Engineering Projects Laboratory
Department of Mechanical Engineering
Massachusetts Institute of Technology
Cambridge, Massachusetts 02139

October 1, 1971

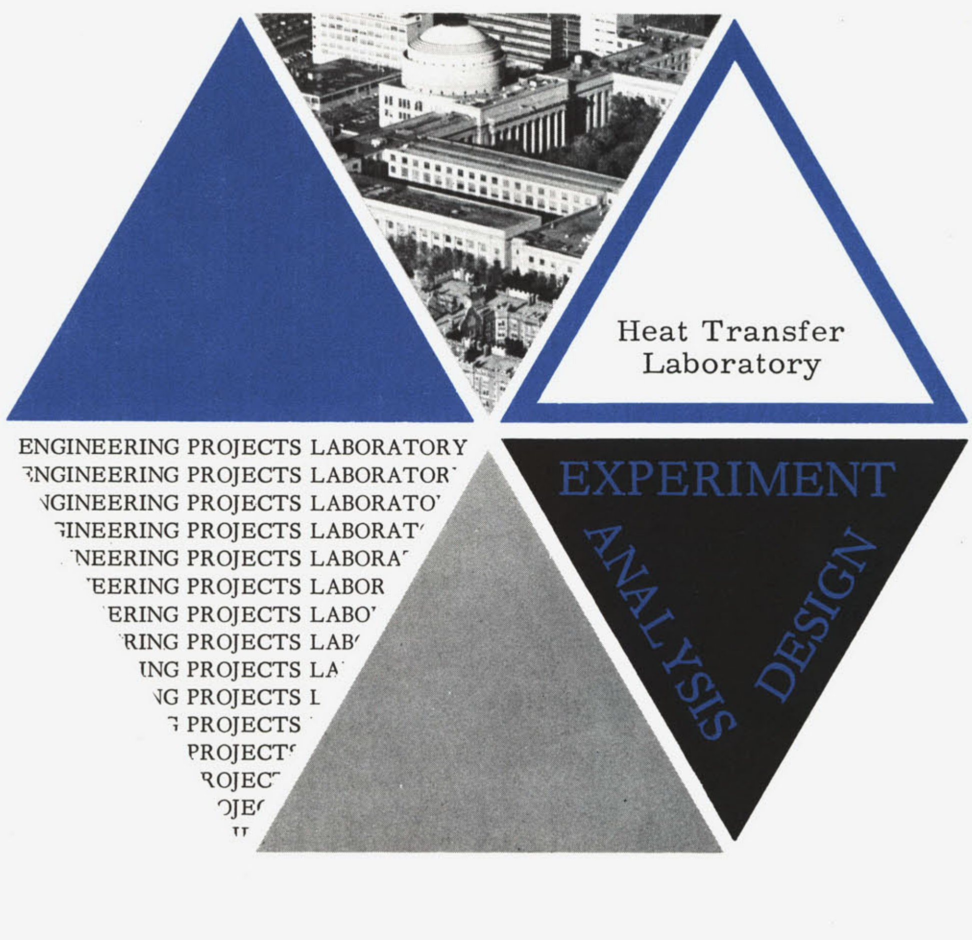

Technical Report No. 72591-75

THE INFLUENCE OF RETURN BENDS ON THE DOWNSTREAM PRESSURE DROP AND CONDENSATION HEAT TRANSFER IN TUBES

by

Donald P. Traviss
Warren M. Rohsenow

Sponsored by:

Technical Committee 1.3

American Society of Heating, Refrigeration, and Air Conditioning Engineers

Contract No. ASHRAE RP63

DSR Project No. 72591-75

October 1, 1971

Heat Transfer Laboratory
Department of Mechanical Engineering
Massachusetts Institute of Technology
Cambridge, Massachusetts 02139

THE INFLUENCE OF RETURN BENDS ON THE DOWNSTREAM PRESSURE DROP AND CONDENSATION HEAT TRANSFER IN TUBES

by

Donald P. Traviss
Warren M. Rohsenow

Massachusetts Institute of Technology

ABSTRACT

The influence of return bends on the downstream pressure drop and heat transfer coefficient of condensing refrigerant R-12 was studied experimentally. Flow patterns in glass return bends of 1/2 to 1 in. radius and 0.315 in. I. D. were examined visually and photographically using a high frequency xenon light source. Local pressure drop and heat transfer measurements were made along a horizontal 14 1/2 ft. test section immediately following the return bend. The refrigerant mass flux ranged from 1.32×10^5 to 4.58×10^5 lbm/hr-ft^2, saturation temperature from 90 to 107°F, and return bend quality from 0.24 to 1.0. The pressure drop and heat transfer data were compared to previous data for condensation without return bends. Effects on the downstream pressure drop and heat transfer were found to be small, if not negligible.

ACKNOWLEDGEMENT

The authors are grateful to ASHRAE Technical Committee TC 1.3 for support of this work.

TABLE OF CONTENTS

INTRODUCTION

A wide variety of vapor-compression refrigeration systems utilized in industry employ condensing equipment in which the refrigerant vapor condenses while flowing inside tubes. This is the case, for example, in evaporative condensers and some water-cooled condensers of the tube-in-tube type. The present investigation is concerned with the heat transfer and pressure drop in condensers, and particularly the effect of return bends on their performance.

The proper design and sizing of condensing equipment requires an accurate knowledge of heat transfer coefficients and associated pressure gradients over a wide range of conditions. In general, these quantites are functions not only of the refrigerant being used, but also of the mass velocity, condensing pressure, condensation rate, vapor quality, and condenser size and configuration. The large number of variables involved indicates not only the difficulty of obtaining sufficient data to cover all the conditions of interest to a design engineer, but also the desirability of devising an efficient and rational way of presenting the data for simplified design calculations.

Two-phase pressure drop and heat transfer are usually interrelated for condensation in tubes. Numerous investigations of two-phase pressure drop in tubes have been reported in the literature. Most of these investigations pertain to straight tubes and fully developed flow.

There are essentially two different mechanisms of condensation in straight tubes. At low mass velocities, laminar film condensation and stratified flow exist. This situation has been examined by Chaddock [1], Chato [2], and Rufer [3] using results from Nusselt [4]. At high mass velocities the liquid refrigerant becomes more evenly distributed in the tube and the mechanism of heat transfer changes. Recently, this case was investigated by Bae [5] and Traviss [6].

Commercial refrigerant condensers, however, do not usually operate under the idealized conditions analyzed in Ref. [1] through [6]. Due to the length of tubing, space limitations, and exterior cooling requirements, the condenser tube usually includes return bends. The refrigerant flow configuration, pressure drop, and heat transfer are modified in the vicinity of a return bend. The purpose of the present investigation is to determine whether the disturbance caused by a return bend is only a localized effect or extends over a significant length of the condenser tube, modifying the heat transfer and pressure drop.

Substantial research has been conducted by many investigators, including White [7], Beij [8], Pigott [9], and Ito [10], in an effort to correlate single-phase pressure drop data for bends. Unfortunately, the results are in substantial disagreement. The recent approach has been to consider the bend as a separate entity responsible for the total increase in pressure caused by its presence. This total increase includes losses due to friction, curvature, and downstream pressure recovery.

In general, a certain minimum number of diameters of straight pipe downstream are necessary for the reestablishment of fully developed straight pipe flow. Ito [10] studied single-phase pressure recovery lengths downstream of bends and showed that full recovery takes place within 50 pipe diameters. Other investigators [11, 12] have indicated that 15 to 20 diameters of straight pipe are adequate for pressure recovery in single-phase flow.

There is less information about two-phase flow through bends, particularly in regard to downstream pressure recovery and heat transfer. Zahn [11] observed that the effect of refrigerant flow in a small-radius glass return bend was the mixing of vapor and liquid and the formation of spray into the entrance of the next tube. Visually there appeared to be little difference between up or down flow through a vertical bank of horizontal tubes. Alves [12] investigated the flow of air-water and oil-water mixtures through a 1-inch glass return bend of 7-inch radius. Alves also measured the pressure drop in the return bend and in the straight sections before and after the bend. The pressure drop data in the straight sections preceeding and following the bend agreed fairly well with the Lockhart-Martinelli correlation [13]. The two-phase pressure drop expressed as L/D due to the return bend was found to be the same order of magnitude as that for single-phase flow.

Fitzimmons [14] measured the single-phase (water) and two-phase (steam-water) pressure drop for 2-inch pipe with contractions, expansions, valves, orifices, and 90° bends. The results indicated that the ratios of two-phase to single-phase pressure drop for various bend radii were insensitive to pressure (800 psia to 1600 psia) and had a maximum value of 2.5. The pressure recovery due to an upstream disturbance (bend) was essentially complete after 55 pipe diameters. Mochan [15] measured the pressure drop of steam-water flow through 75° and 90° bends. The pressure drop in the bends was found to be a function of the dynamic pressure and orientation of the outlet of the bend. If a vertical or inclined section followed the bend, the loss of pressure due to the bend was 2 or 3 times greater for two-phase flow than single-phase flow. If the exit section was horizontal, the two-phase and single-phase pressure losses were approximately equal. The pressure recovery length after the return bend was always less than 100 tube diameters.

Sekoguchi [15] examined the influence of mixers, bends, and exit sections on the horizontal two-phase flow of air and water. He observed that after the bend the pressure decreased more rapidly, followed by less rapid decrease. This region for 90° bends extended over a length of as much as 150 D. Nevertheless, the net effect of a bend on pressure drop appears to be very small. Sekoguchi also correlated the pressure drop in bends using variables analogous to the Lockhart-Martinelli variables for straight pipe flow.

In the present investigation, refrigerant R-12 was condensed in a 3/8 inch O. D. copper tube, located immediately downstream of a glass return bend. High speed photography was used to study the two-phase flow patterns in the return bend. Both the downstream pressure gradient and heat transfer coefficient were measured. In addition, the pressure drop across the return bend was measured. The pressure gradient and heat transfer data were compared with data for fully developed straight tube conditions. On the basis of this information, design recommendations are made.

EXPERIMENT

General Description of the Experimental Apparatus

The basic apparatus is shown schematically in Fig. 1. It consisted of a closed-loop refrigerant flow circuit driven by a mechanical-sealed rotor pump. An electrically heated boiler generated vapor which passed through a flow meter and into the precondenser. After the precondenser, the vapor-liquid mixture flowed through a straight copper tube and into the glass return bend. A 14.5 ft. test section, located immediately after the return bend, was used to determine the local heat transfer coefficients and pressure gradients. Following the test section, all of the refrigerant was condensed to liquid in the aftercondenser, and returned to the boiler by the pump. The pump return line incorporated a filtering-drying element and a commercial sight-glass moisture indicator. Valves in the return line and by-pass loop were used to control the refrigerant flow rate and pressure. Pictures of the experimental apparatus are shown in Fig. 2.

The flow rate of the saturated vapor leaving the boiler was measured by a calibrated variable area rotometer. The precondenser, a sealed shell and coil condenser, was used to control the quality of the refrigerant entering the return bend. The water flow rate into the coil-side of the precondenser was controlled by a gate valve and measured by a rotometer. Inlet and outlet temperatures of the water and refrigerant were also measured. From this information, the refrigerant flow rate, quality, and temperature at the exit of the precondenser were determined.

The two-phase refrigerant flowed from the precondenser into a straight, adiabatic copper tube. The tube was standard 3/8-type L copper tubing, approximately 180 diameters long. A modified Conax PG4-375 packing gland was sweat soldered to the end of the copper tube and another to the inlet of the test section. A metal pin that fit both the inside of the tubes and fittings was used to allign the tubes and fittings in the axial and radial directions before soldering. The end of the tube was allowed to project 1/16 in. into the fitting seal as shown in Fig. 3. When the fitting was tightened the seal compressed around the glass tube and forced the ends of the glass and copper tubes together.

The glass return bend was constructed from 10 mm Pyrex glass tubing. Since the inside diameter of glass tubing varies from lot to lot, the glass tube was carefully selected so that the glass and copper tubes had the same inside diameter (0.315 in.). The bend radius and tube radius were kept as nearly circular as possible. The ends of the return bend were ground flat and the entire bend was annealed. Two different return bends were used: one had a bend radius of 0.5 in., while the other had a bend radius of 1.0 in. The return bend was installed in the vertical position, so that the refrigerant would flow in horizontally at the top and out horizontally at the bottom. The dimensions of the bend are shown in Fig. 3. Pressure taps were installed at points approximately 10 diameters upstream and downstream from the return bend. An enclosure, constructed from 1/2 in. Plexi-glass, was used to shield the return bend from the observer.

The test section was a tube-in tube heat exchanger: the refrigerant flowed through the inner tube and the water flowed countercurrently in the annulus or jacket. The inner tube was a commercial 3/8 in. O. D. (0.315 in. I. D.) continuous copper tube, 14 1/2 ft. long.

Seven brass rings, each incroporating a pressure tap, were soldered to the inner tube at 29 in. intervals. These split the annulus lengthwise into six sections. Heat transfer and pressure drop measurements were made in each of these sections. Adjoining sections of the water jacket were connected in series by flexible hoses to ensure mixing. Two differential thermocouples were located at the inlet and outlet of each jacket for measuring the temperature rise of the water through each section. In addition, two differential thermocouples were located at the first water inlet and the last water outlet in order to check the overall water temperature rise against the sum of the six individual water temperature rises. At the mid-length of the last five sections two thermocouples were installed: one on the outside wall of the condenser tube and one at the centerline of the tube.

The first section after the return bend was instrumented more elaborately than the other sections. This section was equipped with three thermocouples around the outer circumference at the mid-length. The thermocouples were arranged 90° apart at the bottom, side, and top of the tube. Additional thermocouples were installed on the outer tube wall at the bottom of the quarter-lengths and at the centerline of the mid-length. The wall temperature thermocouples were soldered flush to the outer surface of the copper tube; and, as such, did not project into the boundary layer of the coolant. To install the centerline thermocouples, holes were bored into the copper tube and open-ended stainless steel tubes, 0.035 in. O. D., were soldered in the holes. The tip of the stainless steel tube was 1/64 in. short of the copper tube centerline. The thermocouples were then inserted so that the thermocouple beads would be at the centerline of the copper tube. Subsequently, the thermocouples were glued in place with epoxy. All the thermocouples were made of 0.005 in. O. D. nylon-sheathed copper and constantan wire.

Downward-sloping copper tubes connected the pressure taps to a U-tube mercury manometer through a manifold which enabled the measurement of the refrigerant pressure drop through each section. A Bourdon pressure gage, located upstream of the test section, was used to measure the inlet saturation pressure.

Calibrated flow meters were used to measure the flow rate of the water through the precondenser, test section, and aftercondenser. These components were also instrumented with thermocouples at the inlet and outlet of both the refrigerant and water sides. The entire loop was insulated with fiberglass. The heat loss from the test section with zero water flow rate was not measurable within the accuracy of the potentiometer.

Test Procedure

It was desirable to eliminate all possible contaminants before charging the refrigeration loop. The loop was evacuated to 30 in. Hg and filled with dry nitrogen repeatedly to eliminate moisture. Then the system was evacuated and filled with the refrigerant vapor until a pressure of 70 psig. was reached. The refrigerant was then allowed to escape through bleed valves at the aftercondenser, boiler return line, and manometer until the pressure fell to 5 psig. This was repeated twice in order to dilute any traces of non-condensibles in the system. The system was then charged with liquid refrigerant until the sight glass in the boiler showed that the heating elements were covered.

Several parameters, such as water temperature, boiler heat input and flow rate, could be regulated to establish the conditions for a run. The temperature of the water entering the precondenser, test section, and aftercondenser was controlled by mixing hot and cold water feeds. The water temperature, water flow rates, by-pass valve setting, and boiler heat input determined the refrigerant temperature, pressure, and flow rate. During a run, the refrigerant saturation temperature and flow rate were held constant ($\pm$ 4 percent) while the return bend inlet quality was varied in steps from a maximum value of 1.0 to a minimum value of 0.24. After sufficient data had been obtained at one flow level, the refrigerant flow rate was changed to a different value and another series of runs was made. The return bend inlet quality was limited to qualities above 0.24, since a small measurement error in the overall heat balance could result in a significant error in the measured quality for values below 0.20. The data for any run were taken one hour after the system had reached steady state.

After completing a run, pictures and visual observations of the flow patterns in the glass return bend were made. The back of the Plexiglass enclosure for the bend was covered with translucent white paper to diffuse light. A variable frequency xenon light source (General Radio Strobotac, Type 1531-AB) illuminated the background. The flashing-rate range of light source could be varied from 2 to 420 times/second and the flash duration from 1 to 3 μ sec. When the flashing-rate was below the persistence of vision or retina retention limit (approximately 0.1 sec.), periodic flow phenomena such as liquid slugs, waves, and churning could be readily observed. This method was valuable, because the probability of obtaining a truly representative photograph of these flow patterns is low. When the flow was wavy, it was possible to essentially "stop" the flow by properly setting the flashing-rate. Photographs of the flow patterns were also made using a Polaroid camera which simultaneously triggered the strobe lamp.

Data Reduction

An overall heat balance was performed for each run by comparing the heat gained by the water with the heat lost by the refrigerant in the precondenser, test section, and aftercondenser. For all runs, the error was less than 8 percent. The heat flux from the refrigerant was obtained by multiplying the water flow rate by the water temperature rise and specific heat. Using the thermal conductivity of the inner tube, dimensions of the inner tube, and heat flux, the temperature drops across the tube wall were calculated. From this information, the inside wall temperatures were determined. The refrigerant qualities at the inlet to the return bend and midpoints of the six sections were determined from a heat balance using the thermodynamic properties of the refrigerant, refrigerant flow rate, and heat gain of the water. The condensation heat transfer coefficient was obtained by dividing the average heat flux for a section by the difference between the vapor temperature. The pressure gradient was calculated by dividing the pressure drop across one section by the length of that section.

The preceding calculations were performed using an IBM model 1130 computer. Thermodynamic properties used in the calculations were evaluated from a piece-wise-linear curve fit of values found in Ref. [17, 18]. The computer program is presented in Appendix 1.

During each experimental run, the pressure drop across the return bend was measured using a manometer. The manometer readings were corrected for the hydrostatic head difference between the inlet and outlet pressure taps. Corrections were also made for the pressure drop in the tube segments between the bend centerline and pressure taps using the fully-developed pressure gradient data from other runs at the same conditions. The return bend pressure drop data were then converted into equivalent lengths of straight tube required for the same two-phase pressure drop.

RESULTS

Twenty-four experimental runs were made using refrigerant R-12 over a range of saturation temperatures from 90°F (114.5 psia) to 107°F (145.1 psia), mass fluxes from 1.32×10^5 to 4.58×10^5 lbm/hr-ft^2, and return bend qualities from 0.24 to 1.0. The absolute value of the maximum heat balance error for all the runs was 8 percent. The tabulated data are presented in Appendix 2 with the runs ordered (U-1 through U-24) according to increasing mass flux and return bend quality. The experiments were performed at three different mass flux levels: 1.35×10^5, 2.75×10^5, and 4.55×10^5 lbm/hr-ft^2. At each mass flux level, tests were made using a 1/2 and 1 in. radius return bend. In addition, data were obtained for four to six inlet qualities at each of the mass flux levels and for each return bend radius.

The experiment was designed so that the experimental data would be representative of the conditions in industrial and commercial refrigeration and air-conditioning equipment. One apparent anomaly is that the inlet tube to the return bend and the return bend were adiabatic or insulated. In most condensers, the inlet tube and return bend would be diabatic or transfering heat. Before the return bend runs were made, it was experimentally determined that an adiabatic length did not measureably affect the downstream heat transfer and pressure drop. Using a straight test section (which was divided into six zones, as previously described) heat transfer and pressure drop data were taken with condensation occurring over the entire test section length. Subsequently, the water flow through one of the zones in the middle of the test section was turned off.

Heat transfer and pressure drop data were then obtained at the same conditions as before, but with an adiabatic zone in the middle of the test section. The heat transfer data for two of these experiments are shown in Fig. 4. These two runs, with a straight test section inlet and no return bend, are denoted as runs S-1 and S-2. The upstream and downstream heat transfer coefficients are virtually the same, with or without an intervening adiabatic section.

The heat transfer and pressure drop in two-phase flow are inextricably related to the two-phase flow configuration or flow regime. From experimental determined qualities, flow rates, and saturation temperature. Baker flow regime parameters [19] were calculated for conditions in the return bend, and also for the downstream conditions in the test section. These data are shown in Fig. 5. The data points on Fig. 5 represent the Baker parameters as calculated at the return bend for a particular run number, and the downstream conditions are depicted by the lines. It should be noted that for a specific mass flux and saturation temperature, all of the flow regime states will be specified by a single line. On the basis of the Baker flow regime map, the flow regimes at the return bend inlet were dispersed or annular at mass fluxes of 4.55×10^5 lbm/hr-ft^2, annular or slug at mass fluxes of 2.75×10^5 lbm/hr-ft^2, and annular at mass fluxes of 1.35×10^5 lbm/hr-ft^2.

During each run, the flow patterns in the glass return bend were also observed and photographed. Typical photographs of these flow patterns for different mass fluxes and qualities are presented in Fig. 6. The photographs and flow visualization revealed a zone of mixing near the midpoint of the bend. If the flow was stratified or semi-annular, the liquid separated from the tube wall and switched to the opposite side. A similar behavior was also observed in the annular and misty flow regimes: the liquid was observed to migrate to the outer radius and the vapor to the inner radius. Secondary flows that tend to sweep liquid from the outer radius towards the inner radius were not observed. Another observation was that the flow patterns at the inlet and exit of the return bend were not substantially different. When the flow was stratified or semi-annular at the return bend inlet, the flow at the exit appeared to be similar, but with a more wavy liquid-vapor interface. Annular and annular-dispersed flow also appeared to be the same at the return bend inlet and outlet. However, small increases in entrainment are difficult to visually detect.

A comparison of the photographs of Fig. 6 and the corresponding run numbers, as calculated and plotted on Fig. 5, is interesting. The photographs agree with the Baker flow regime map for the higher mass fluxes of 2.75×10^5 and 4.55×10^5 lbm/hr-ft^2. However, at the lower mass fluxes of 1.35×10^5 lbm/hr-ft^2, the photograph and observations indicate stratified or semi-annular flow while the Baker map predicts annular flow. The transition from annular to wavy or stratified flow should not be represented by a line as on the Baker map, but by a broad band. The authors have observed in other flow regime investigations [20] with refrigerant R-12 flow through a horizontal tube that the transition was gradual and began at values of G_v/λ as large as 2×10^4 lbm/hr-ft^2, which is considerably higher than the Baker map predicts. This has also been substantiated by other investigators [21].

The pressure drop in the test section was measured over six increments of 92 tube diameters. The first pressure tap was located approximately 10 diameters downstream of the return bend. The refrigerant mass flux and saturation were held constant, and a series of runs were made with different inlet or return bend qualities. Each particular series of runs was then plotted on the same graph. In this manner, a reference of fully developed conditions was inherent in the graph: the pressure gradient over the last half of the test section (276 tube diameters) should be fully developed. These graphs of pressure gradient vs. quality are presented in Fig. 7 through Fig. 11 for bend radii of 1/2 and 1 inch. In general, there appears to be a negligible amount of pressure recovery in the test section downstream of the return bend. The pressure gradient in the first downstream increment does not deviate significantly ($\pm$ 10 %) from the fully developed pressure gradient.

The downstream heat transfer coefficients were also determined in the six test section zones or increments. These data are presented in Fig. 12 through Fig. 16. The heat transfer coefficients are plotted as a function of quality at constant refrigerant mass flux and saturation temperature. From wall temperature measurements, the circumferential temperature variation of the tube wall was always found to be less than 10 percent of the saturation and wall temperature difference. Thus, the high thermal conductivity of the copper tube resulted in an essentially constant wall temperature in the circumferential direction.

The heat transfer data, like the pressure gradient data, do not exhibit any downstream effects due to the return bend. However, it should be noted that data scatter and reproduciability might mask changes of 10 percent or less. In any case, the effect is quite small over the range of experimental conditions considered. Another option considered was to subdivide the first test zone (with a length of 92 tube diameters) into two or three zones in order to obtain more locaiized measurements. This would offer better information in theory; but the instrumentation is difficult, if not inaccurate, due to entrance effects and small temperature differences on the water-side of the test section.

The experimental data from this investigation were compared to the analysis and supporting data of Ref. [6]. Ref. [6], which is briefly described in Appendix 3, pertains to forced-convection condensation of R-12 in a horizontal with no return bends; and, consequently, provides a good basis for comparison. The data points in Fig. 17 represent measurements made for runs U-5 through U-14 and U-19 through U-24 in the first zone of the test section, immediately following the return bend. Hence, these data points should be indicative of the maximum return bend influence on downstream condensation. The agreement of these data with the analysis and supporting data (the solid line for $F(\chi_{tt}) < 1$ and the dotted line for $F(\chi_{tt}) > 1$) of Ref. [6] is good. Thus, the return bend again has no observable effect on the downstream heat transfer. The data from runs U-1 through U-4 and U-15 through U-18 are similarly plotted in Fig. 18. The data of Fig. 18 were taken at a refrigerant mass flux of 1.35×10^5 lbm/hr-ft^2, while the data of Fig. 17 were taken at mass fluxes ranging from 2.5×10^5 to 4.6×10^5 lbm/hr-ft^2.

The data of Fig. 18 are significantly higher than the forced-convection condensation analysis predicts, because the minimum mass flux for which the annular flow model is valid is around 1.35×10^5 lbm/hr-ft^2. Thus, the anomaly at low mass fluxes is due to a flow regime transition. As previously discussed, the flow regime was stratified or semi-annular with small waves, and occurred with or without a return bend. At the lower mass flux level, the condensing refrigerant was in a transition region between stratified, laminar film condensation and annular forced-convection condensation. The heat transfer coefficients for the low flow rate runs were calculated using both the methods of Ref. [3] and [6]. The two methods gave approximately the same values for the heat transfer coefficient, but these values were appreciably lower (50 percent) than the experimental values. Thus in the transition region (as previously defined) the stratified, laminar film condensation model [1, 2, 3] or the annular forced-convection condensation model [5, 6] will give a low estimate of the heat transfer coefficient.

During each run, the pressure drop across the return bend was measured, corrected, and expressed as equivalent straight tube lengths required for the same adiabatic, two-phase pressure drop. The measurement and data reduction techniques were explained in the section entitled Experiment. Generally, the pressure drop across a horizontal return bend includes friction, curvature, and pressure recovery effects. In the present experiment, there was also a gravitational pressure drop component or a pressure rise due to the vertical orientation of the bend. The algebraic sum of the pressure drop components, the pressure drop measured by the manometer, was very small. Since the measured pressure drops, after corrections, were of the same order as the manometer sensitivity, the data are not reported. The pressure drop algebraically increased with increasing mass flux, increasing quality, and decreasing bend radius. A maximum pressure drop of 40 equivalent tube diameters occurred for run U-13, and a minimum pressure drop of -15 equivalent tube diameters occurred for run U-15.

CONCLUSIONS

1. For moderate condensation rates, the pressure drop and heat transfer coefficient in the downstream portion of a condenser tube are the same whether the preceding section is adiabatic or diabatic.

2. Within the range of experimental conditions, the effect of a return bend on the downstream pressure drop and heat transfer coefficient is negligible when averaged over a length of 90 tube diameters or more.

3. When disturbed by the presence of a return bend, the refrigerant two-phase flow pattern appears to readjust very rapidly.

4. The flow regime transition from annular to stratified flow occurs over a fairly wide range, and, consequently, it is not accurately predicted by a single line as shown on the Baker flow regime map.

5. The heat transfer coefficient in the transition region between annular and stratified-wavy flow is higher than that for stratified, laminar film condensation or annular, forced-convection condensation.

REFERENCES

1. Chaddock, J. B., "Film Condensation of Vapor in Horizontal Tubes," Sc. D. Thesis, M. I. T. (1955), also in Refrigeration Engineering, Vol. 65, No. 4, p. 36 (1957).

2. Chato, S. C., "Laminar Condensation Inside Horizontal and Inclined Tubes," ASHRAE Journal, Vol. 4, No. 2 (1962).

3. Rufer, C. and S. P. Kezios, "Analysis of Two-Phase One Component Stratified Flow with Condensation," Journal of Heat Transfer, Trans. ASME, Series C, Vol. 88, No. 3 (1966).

4. Nusselt, M., "Die Oberflachen Kondensation Des Wasserdampfes," Seitschrift des Vereines Deutscher Ingenieure, Vol. 60, No. 541 (1916).

5. Bae, S., J. S. Maulbetsch and W. M. Rohsenow, "Refrigerant Forced-Convection Condensation Inside Horizontal Tubes," Department of Mechanical Engineering, Heat Transfer Laboratory Report No. DSR 72591-71, M. I. T. (1970).

6. Traviss, D. P., A. B. Baron and W. M. Rohsenow, "Forced-Convection Condensation Inside Tubes," Department of Mechanical Engineering, Heat Transfer Laboratory Report No. DSR 72591-74, M. I. T. (1971).

7. White, C. M., "Fluid Friction and Its Relation to Heat Transfer," Trans. Inst. Chemical Engineers, Vol. 10, p. 66 (1932).

8. Beij, K. H., "Pressure Losses for Fluid Flow in 90° Bends," J. Research of National Bureau of Standards, Vol. 21, pp. 1-18, Research Paper No. 1110 (1938).

9. Pigott, R. J. S., "Losses in Pipe and Fittings," Trans. ASME, Vol. 79, pp. 1767-1783 (1957).

10. Ito, H., "Pressure Losses in Smooth Pipe Bends," J. Basic Engineering, Trans. ASME, Series D, Vol. 82, pp. 131-143 (1960).

11. Zahn, W. R., "Flow Conditions when Evaporating Refrigerant-22 in Air Conditioning Coils," ASHRAE Trans., 72, Part I, pp. 82-89 (1966).

12. Alves, G. F., "Co-Current Liquid-Gas Flow in a Pipe Contractor," Chem. Engg. Prog., Vol. 50, pp. 449-456 (1954).

13. Lockhart, R. W. and R. C. Martinelli, "Proposed Correlation of Data for Isothermal Two-Phase Two Component Flow in Pipes," Chem. Engg. Prog., Vol. 45, No. 1, p. 39 (1949).

14. Fitzimmons, D. E., "Two-Phase Pressure Drop in Piping Components," General Electric (Hanford), Report HW-80970, Rev. 1 (1964).

15. Kutateladze, S. S., Ed., Problems of Heat Transfer and Hydraulics of Two-Phase Media, Pergamon Press, pp. 327-384 (1969).

16. Rhodes, R. and D. S. Scott, Editors, Co-current Gas-Liquid Flow, Plenum Press, New York, pp. 109-144 (1969).

17. American Society of Heating, Refrigeration, and Air-Conditioning Engineers, ASHRAE Handbook of Fundamentals, First Ed., pp. 213-224 (1967).

18. E. I. du Pont de Nemours & Co., "Thermodynamic Properties of Freon-12," Wilmington, Deleware (1956).

19. Baker, O., "Simultaneous Flow of Oil and Gas," Oil and Gas Journal, Vol. 53, pp. 185-195 (1954).

20. Traviss, D. P. and W. M. Rohsenow, "Flow Regimes of Horizontal Two-Phase Flow with Condensation," Department of Mechanical Engineering, Heat Transfer Laboratory Report No. DSR 72591-76, M. I. T. (1971).

21. Soliman, H. M. and N. Z. Azer, "Flow Patterns During Condensation Inside a Horizontal Tube," Preprint for ASHRAE Semiannual Meeting in Philadelphia, Pa., January 24-28 (1971).

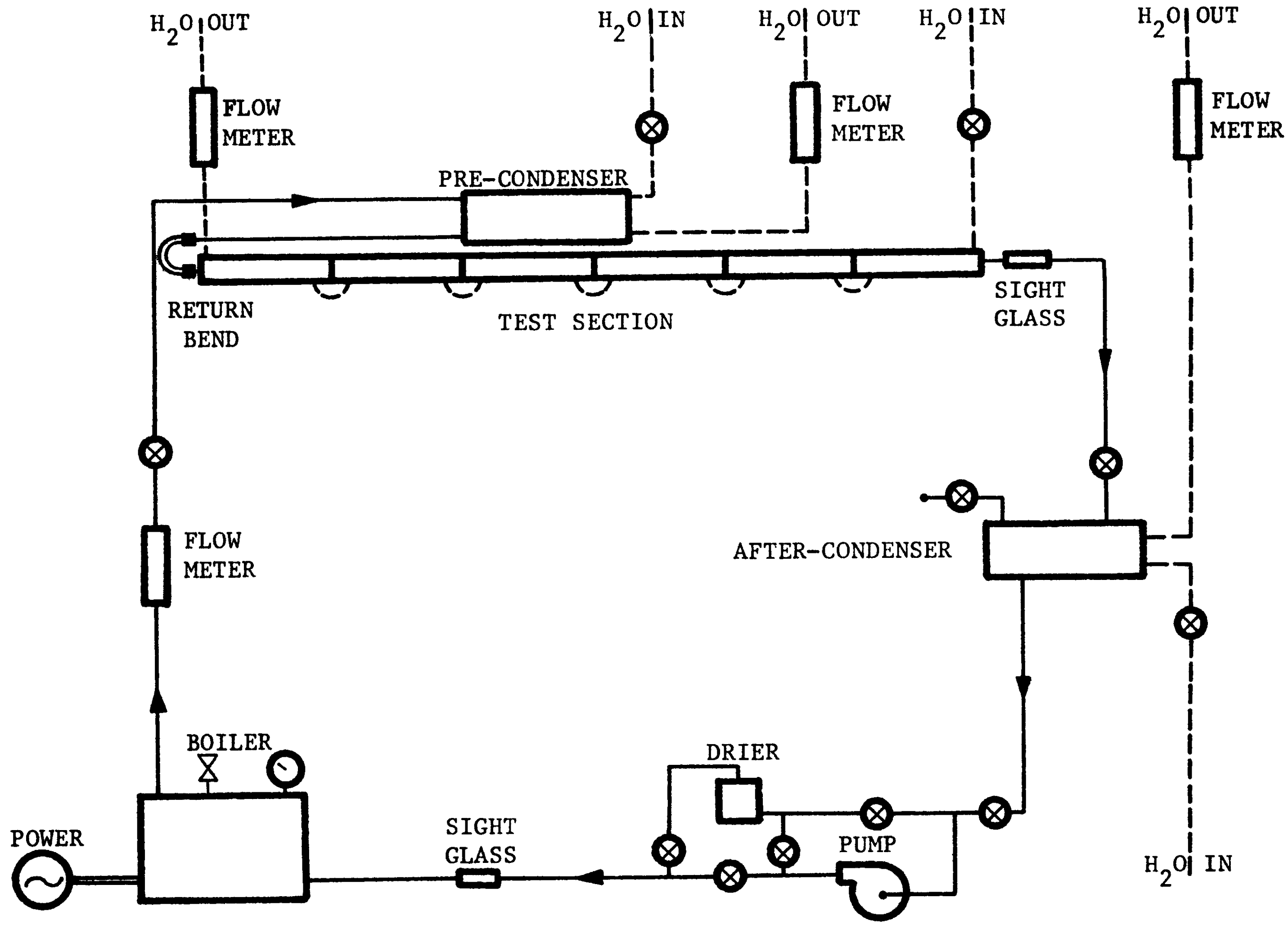

FIGURE 1 SCHEMATIC DIAGRAM OF APPARATUS USED FOR STUDY OF RETURN BEND EFFECTS

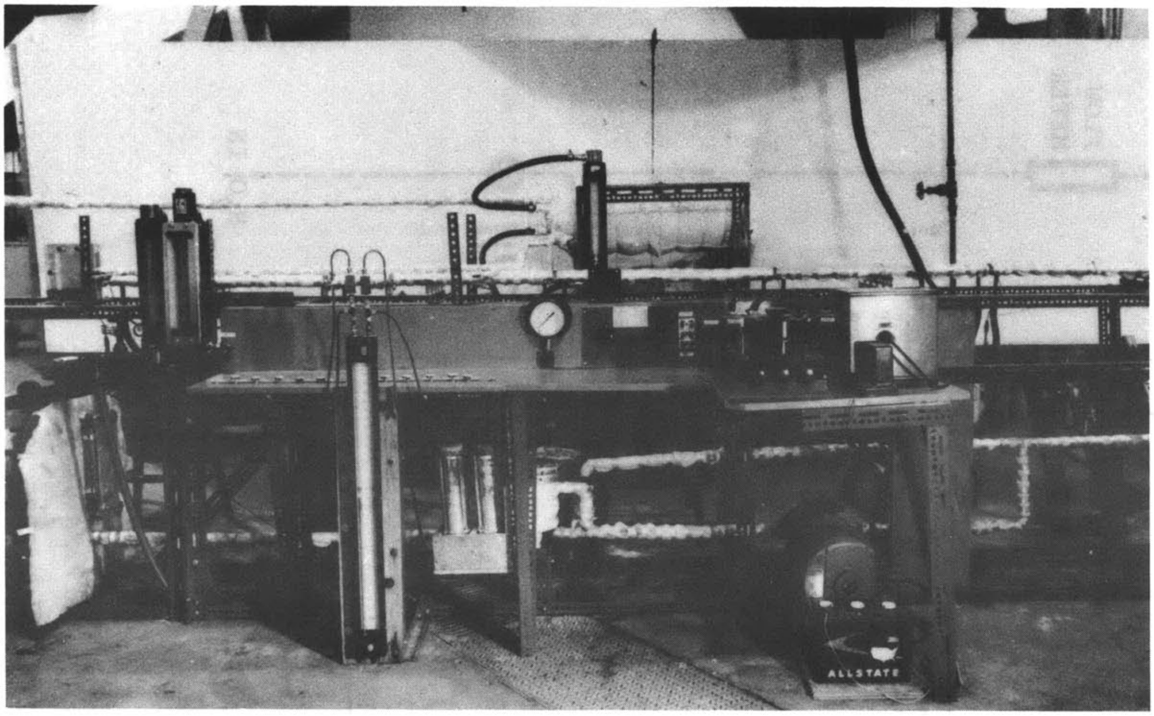

FRONT VIEW

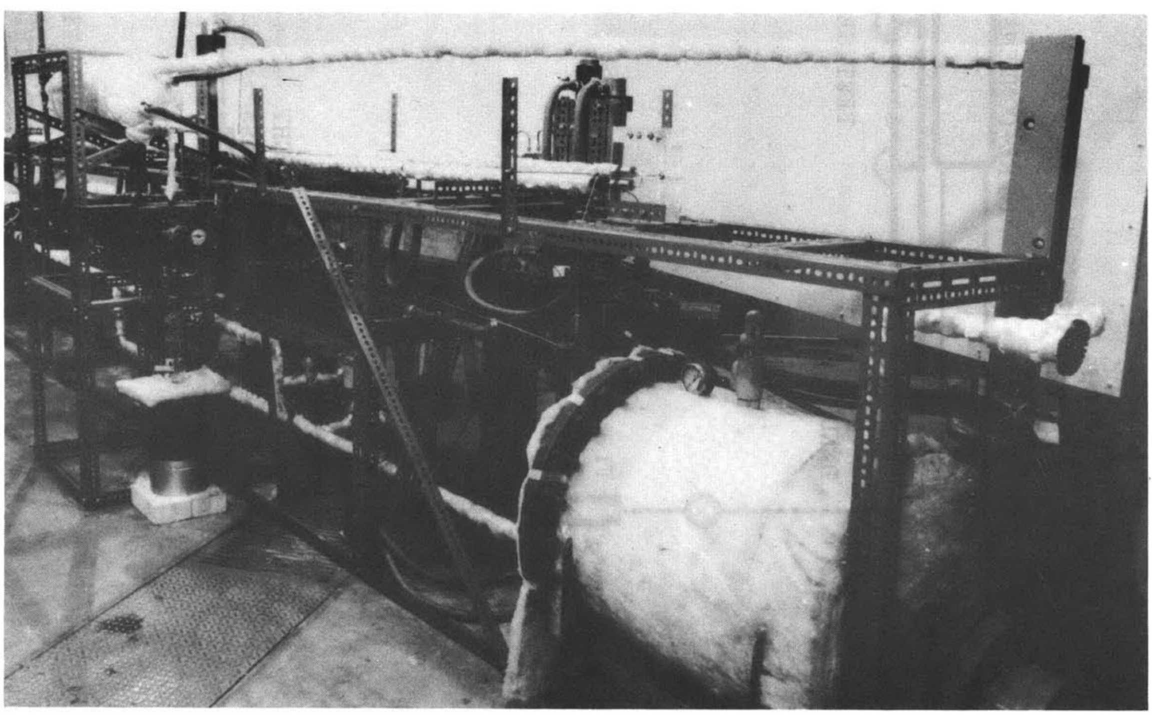

REAR VIEW

FIGURE 2 EXPERIMENTAL APPARATUS

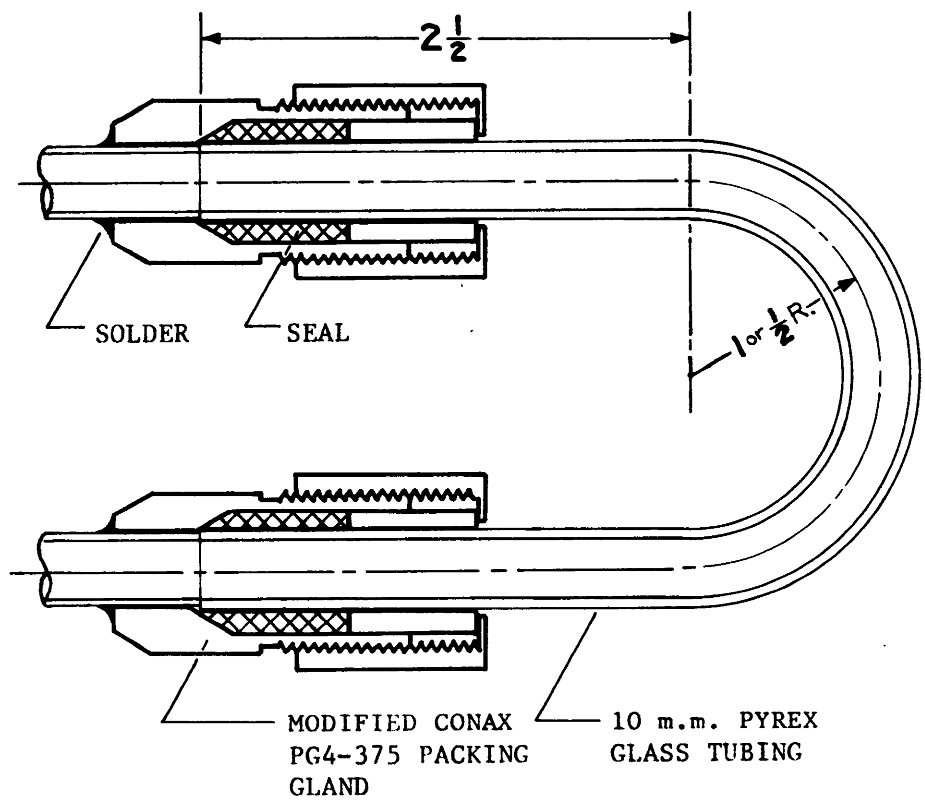

FIGURE 3 RETURN BEND ASSEMBLY

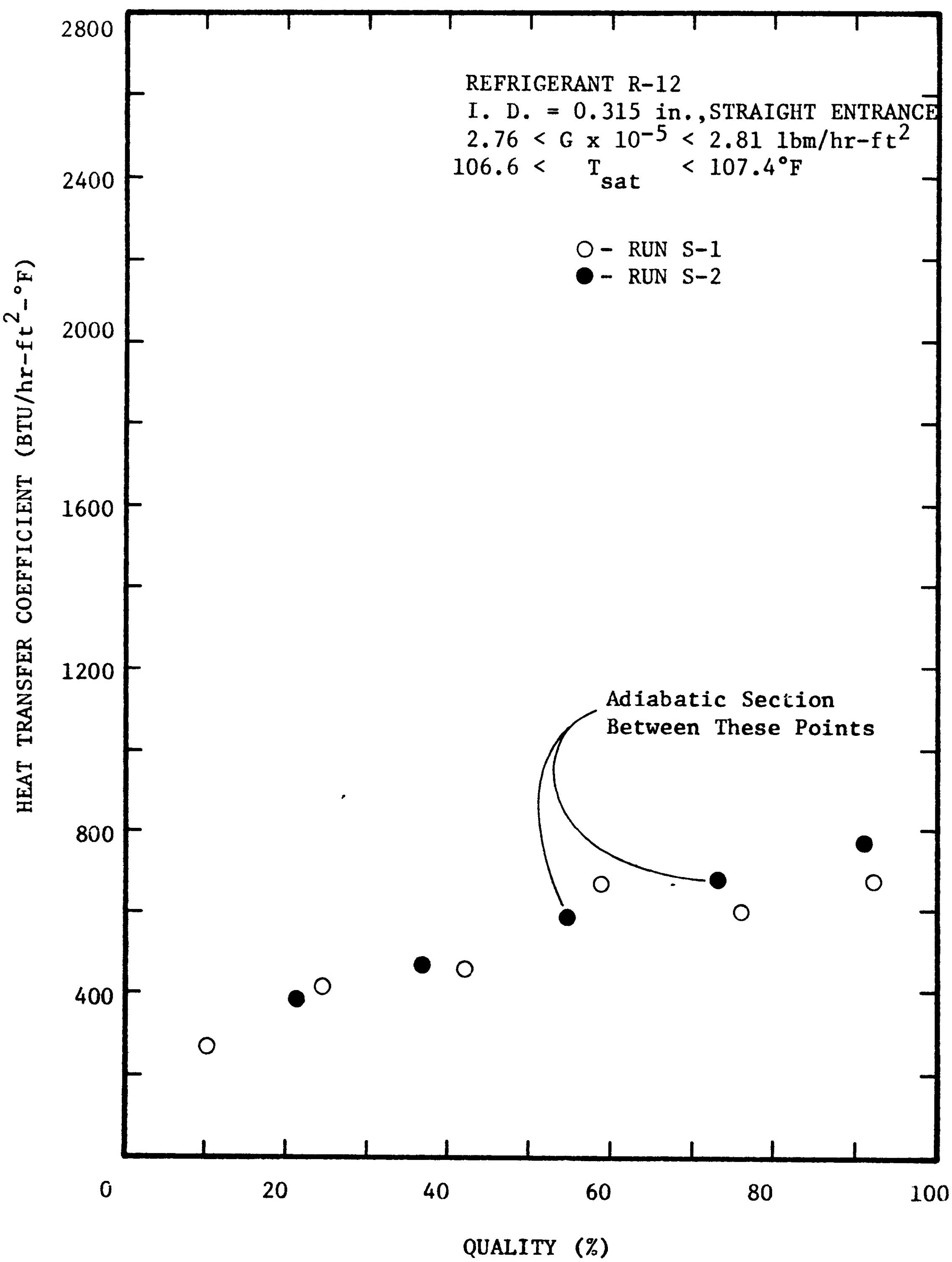

FIGURE 4 HEAT TRANSFER COEFFICIENT vs. QUALITY

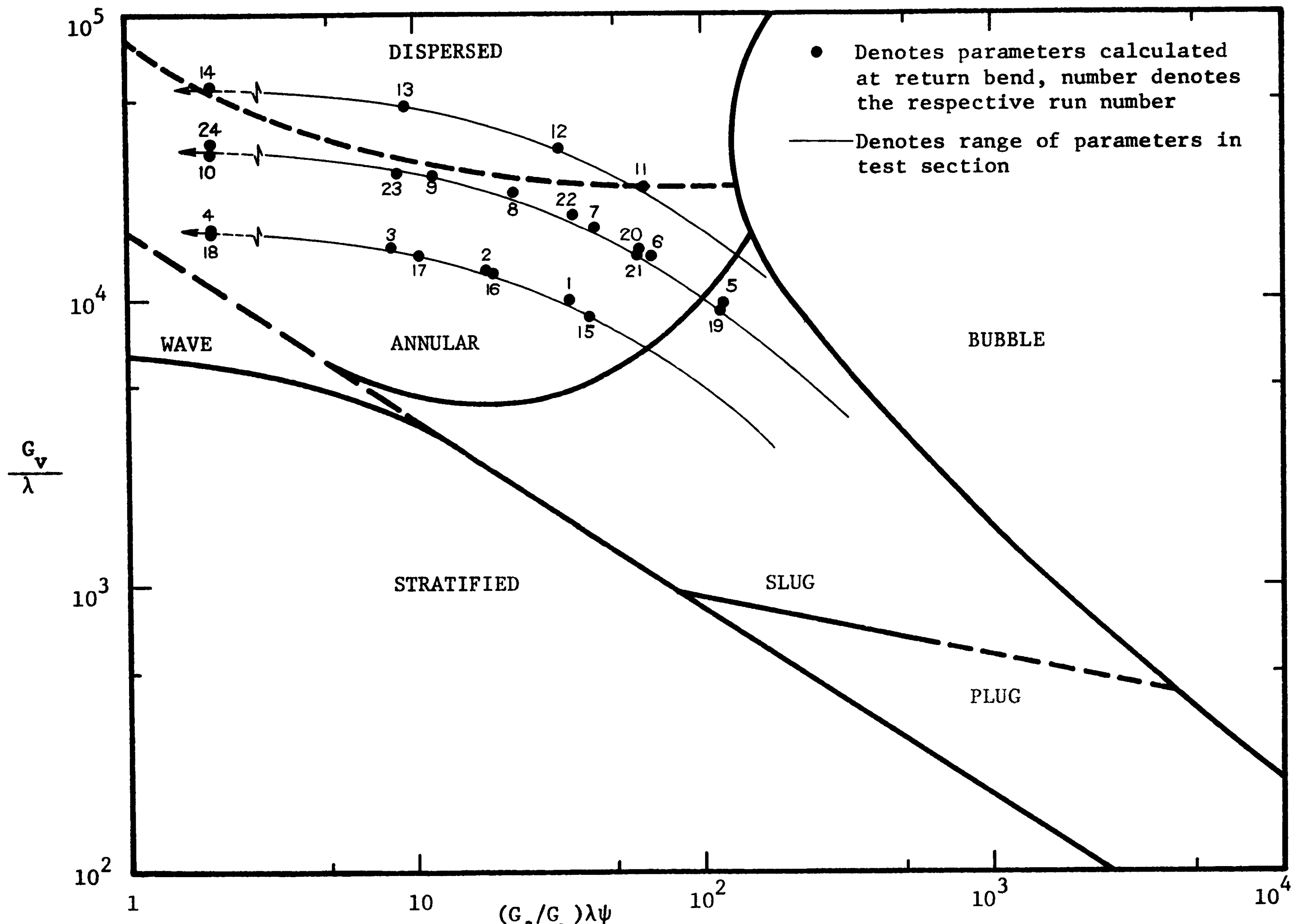

FIGURE 5 BAKER FLOW REGIME MAP FOR RETURN BEND AND DOWNSTREAM CONDITIONS

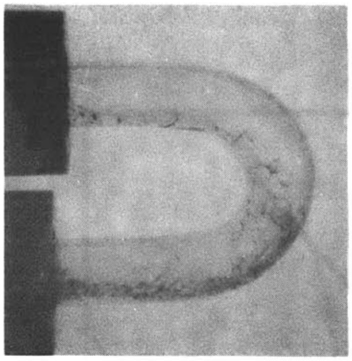

$G = 1.41 \times 10^5$ lbm/hr-ft^2
$x = 0.51$ Run U-1

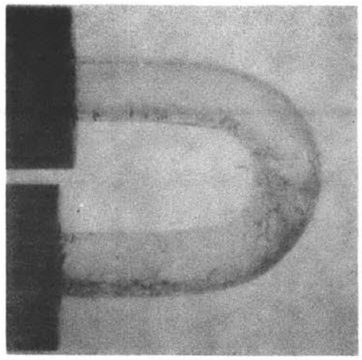

$G = 1.36 \times 10^5$ lbm/hr-ft^2
$x = 0.68$ Run U-2

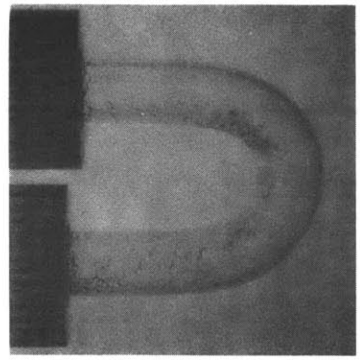

$G = 1.37 \times 10^5$ lbm/hr-ft^2
$x = 0.82$ Run U-3

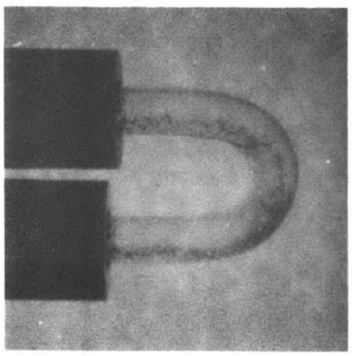

$G = 2.69 \times 10^5$ lbm/hr-ft^2
$x = 0.40$ Run U-6

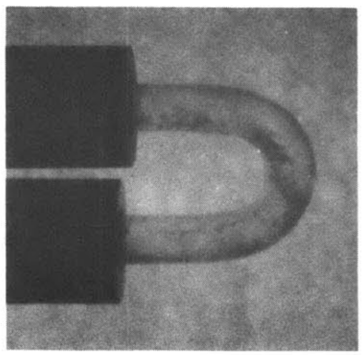

$G = 2.81 \times 10^5$ lbm/hr-ft^2
$x = 0.67$ Run U-8

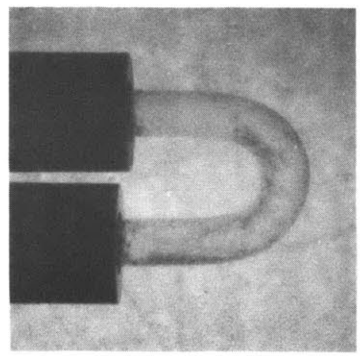

$G = 2.74 \times 10^5$ lbm/hr-ft^2
$x = 0.79$ Run U-9

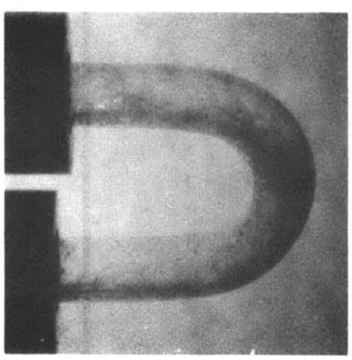

$G = 4.58 \times 10^5$ lbm/hr-ft^2
$x = 0.41$ Run U-11

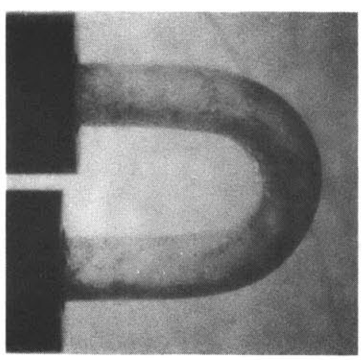

$G = 4.53 \times 10^5$ lbm/hr-ft^2
$x = 0.57$ Run U-12

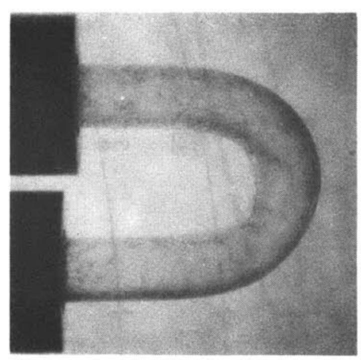

$G = 4.57 \times 10^5$ lbm/hr-ft^2
$x = 0.83$ Run U-13

FIGURE 6 FLOW CONDITIONS IN A 1/2 IN. RADIUS RETURN BEND AT DIFFERENT MASS FLUXES AND QUALITIES

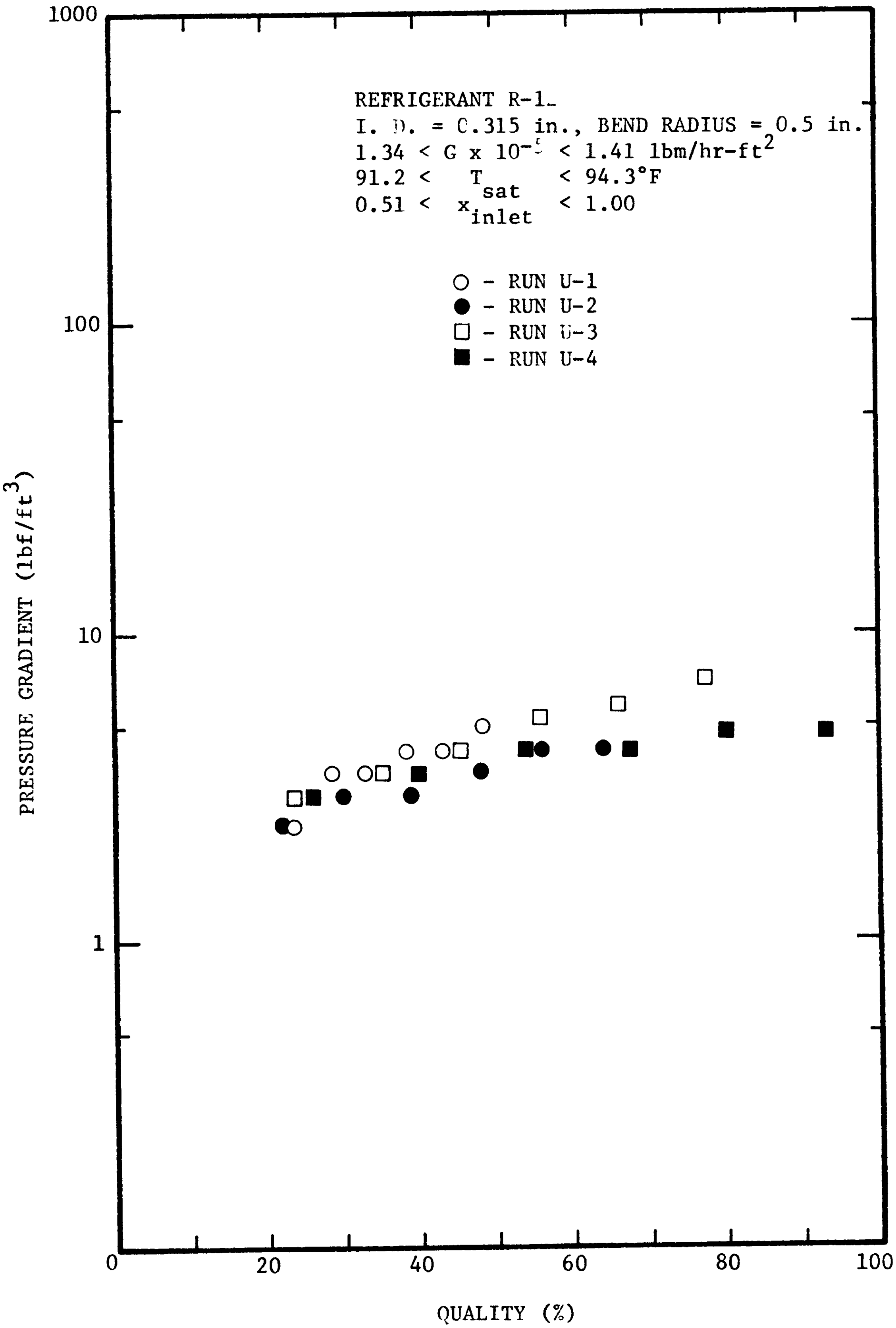

FIGURE 7 DOWNSTREAM PRESSURE GRADIENT vs. QUALITY

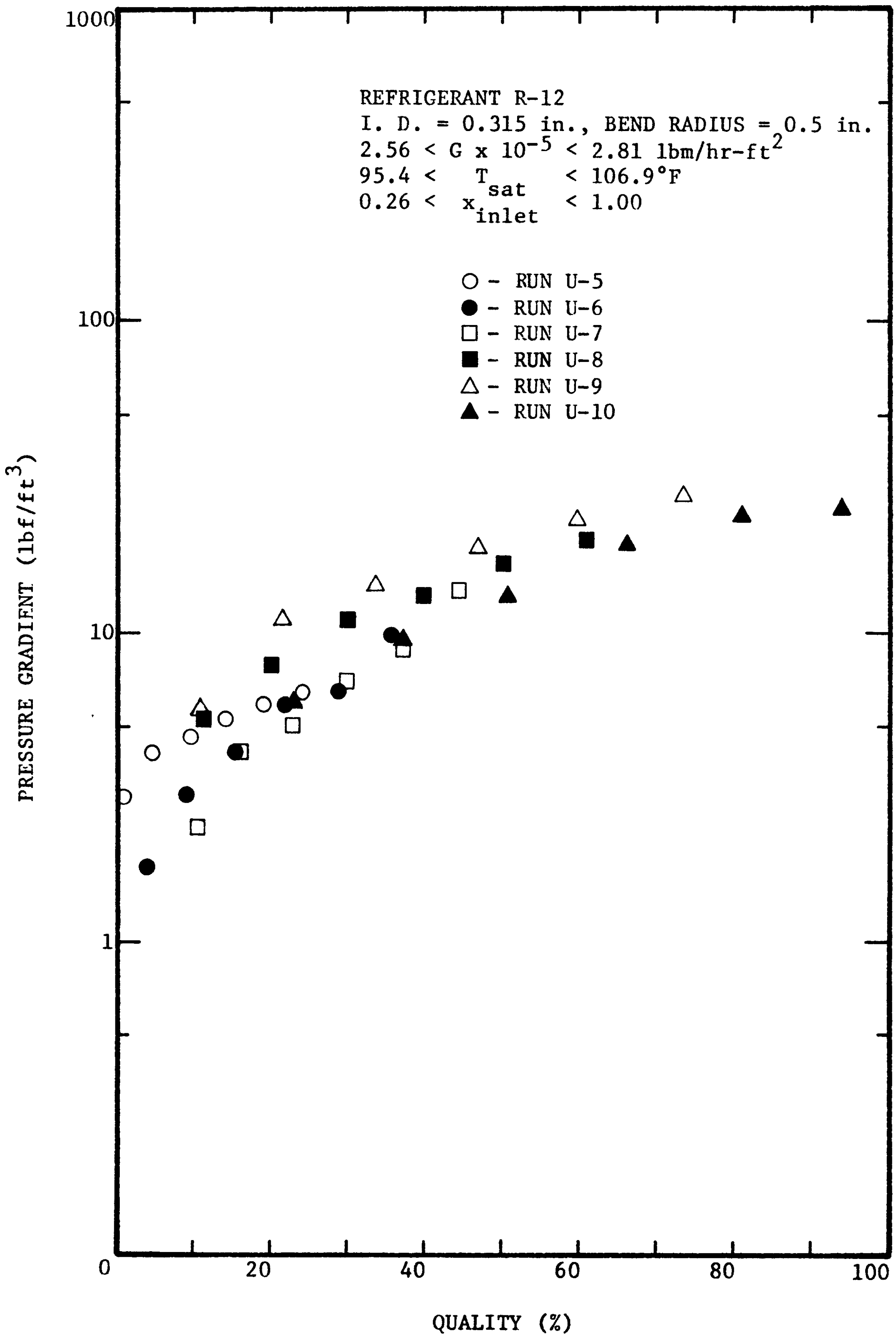

FIGURE 8 DOWNSTREAM PRESSURE GRADIENT vs. QUALITY

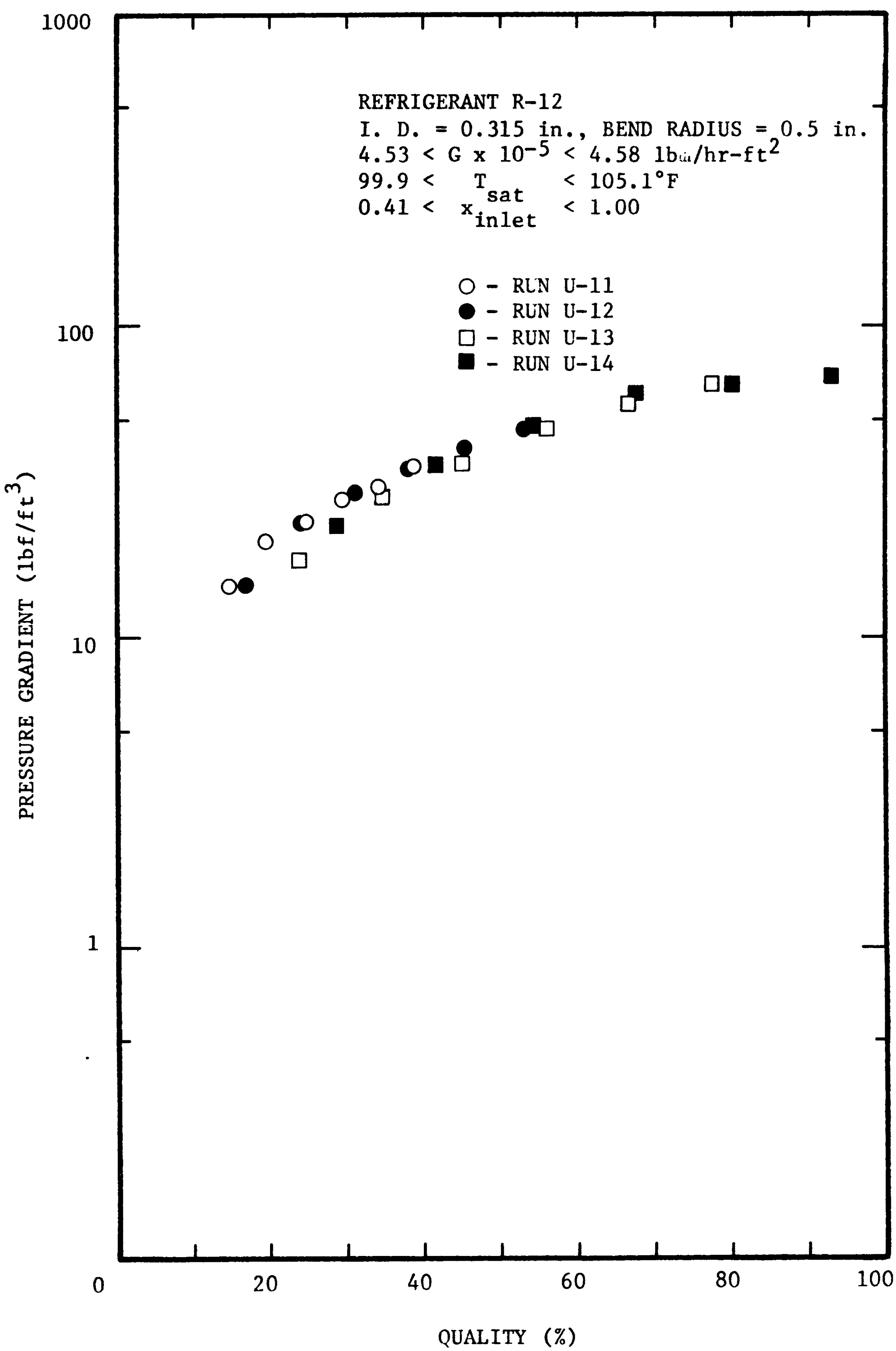

FIGURE 9 DOWNSTREAM PRESSURE GRADIENT vs QUALITY

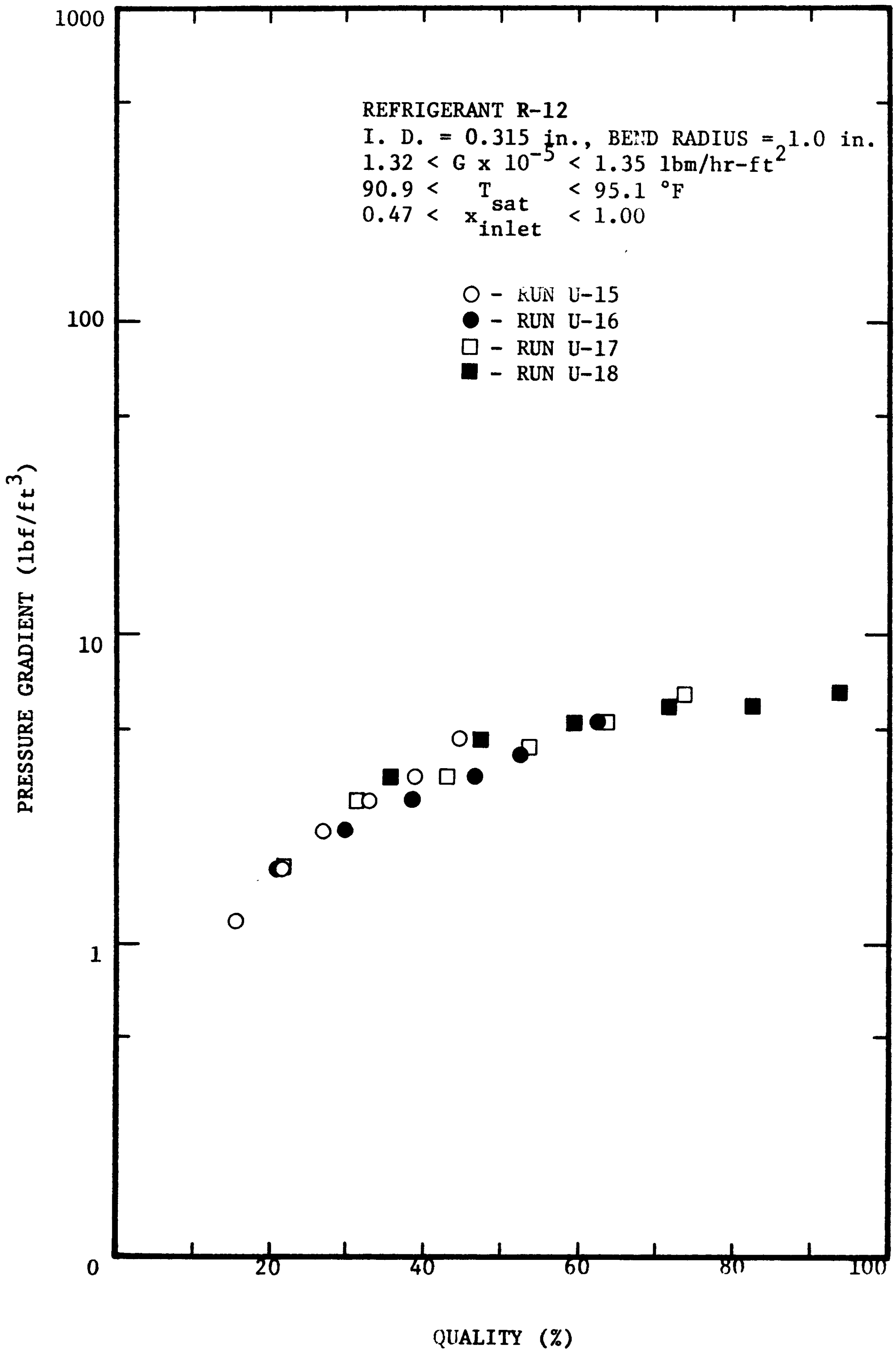

FIGURE 10 DOWNSTREAM PRESSURE GRADIENT vs. QUALITY

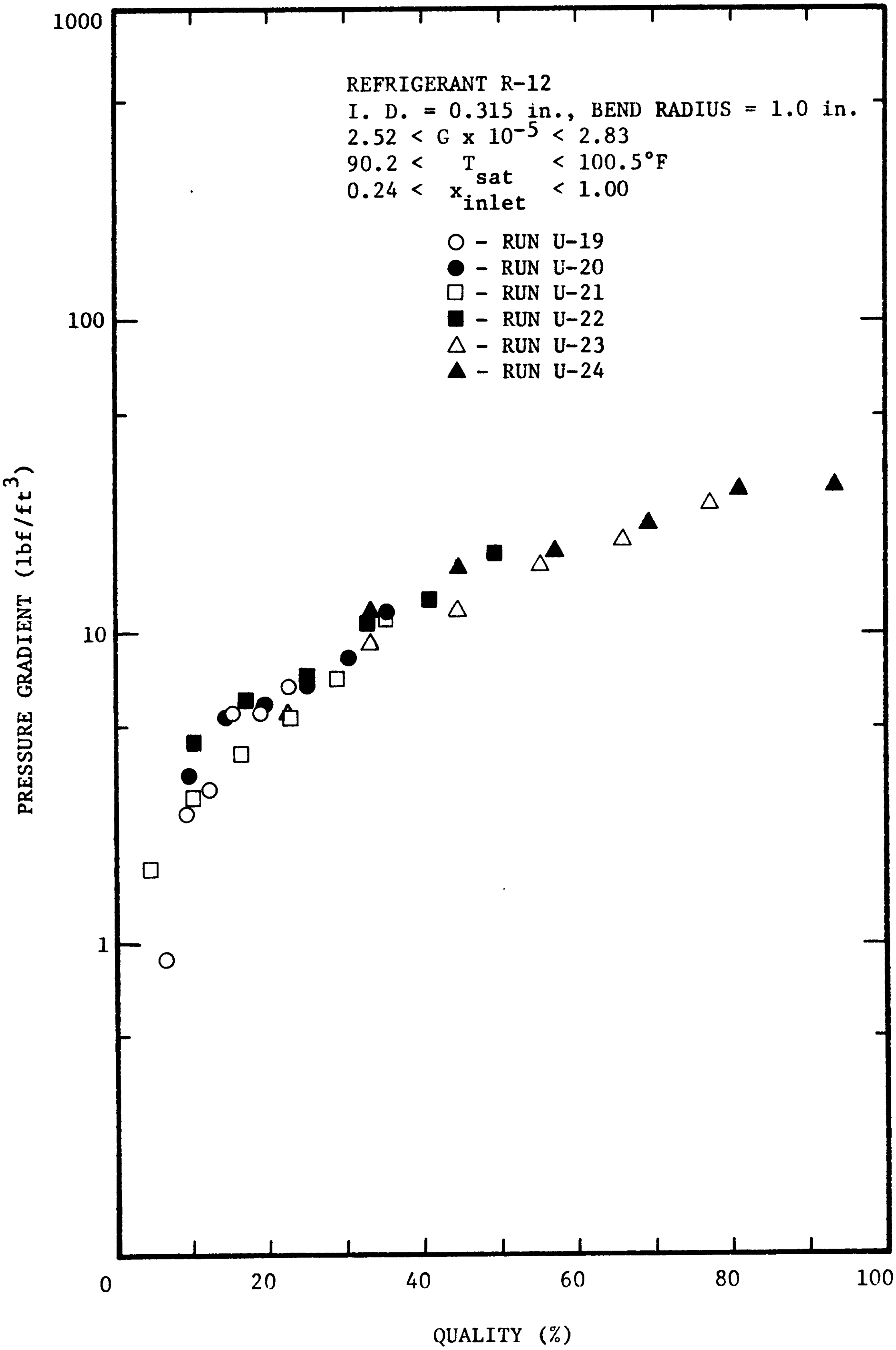

FIGURE 11 DOWNSTREAM PRESSURE GRADIENT vs. QUALITY

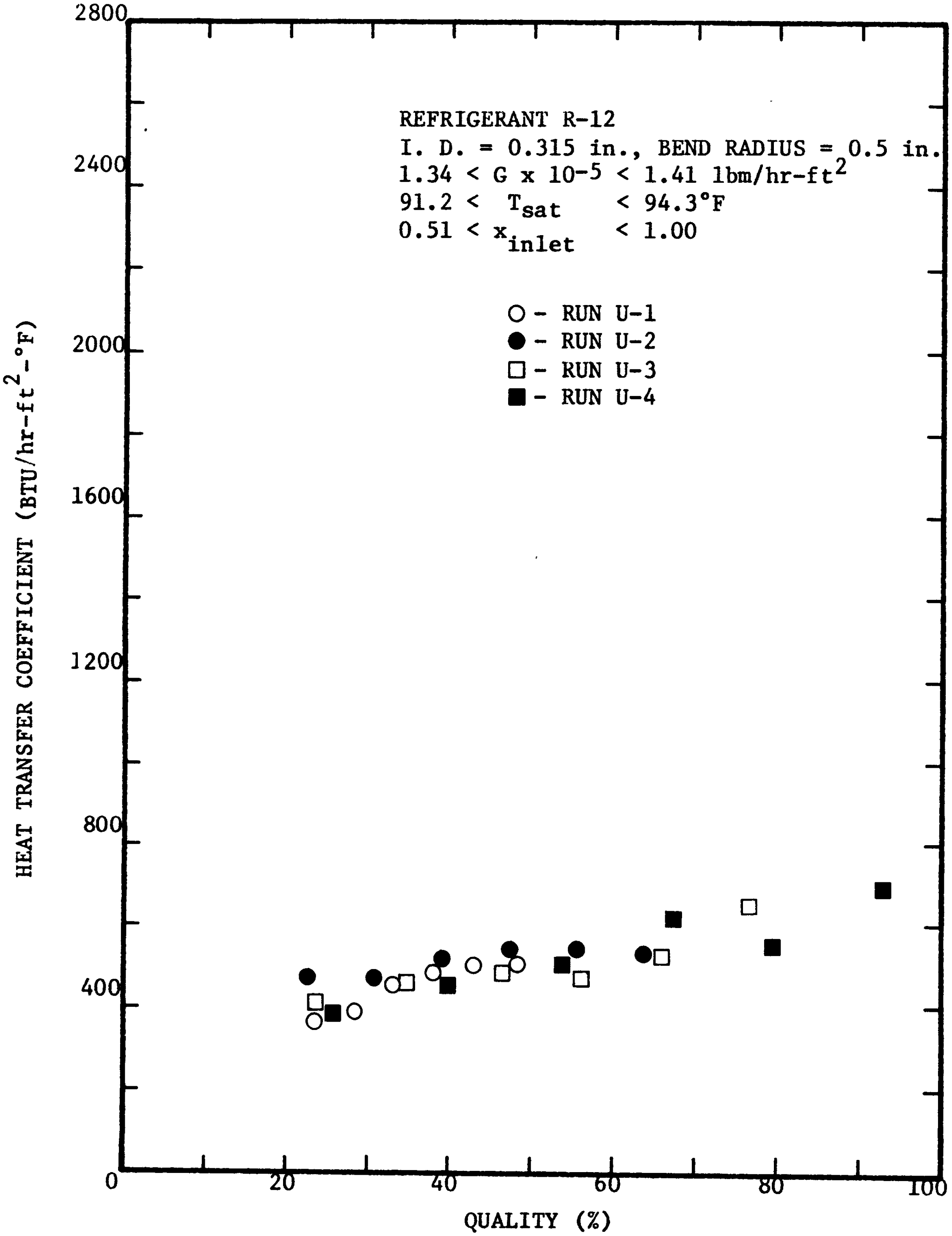

FIGURE 12 DOWNSTREAM HEAT TRANSFER COEFFICIENT vs. QUALITY

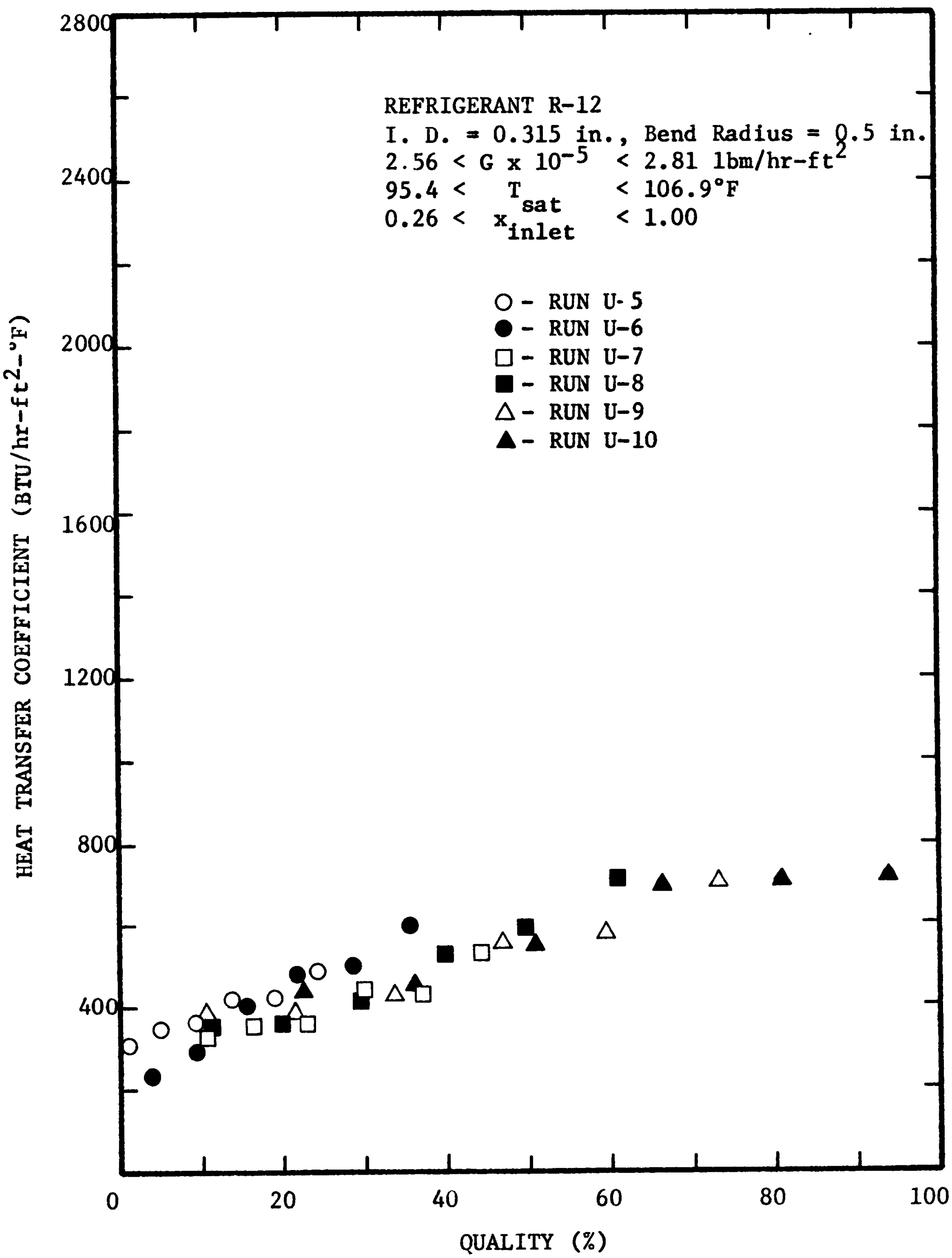

FIGURE 13 DOWNSTREAM HEAT TRANSFER COEFFICIENT vs. QUALITY

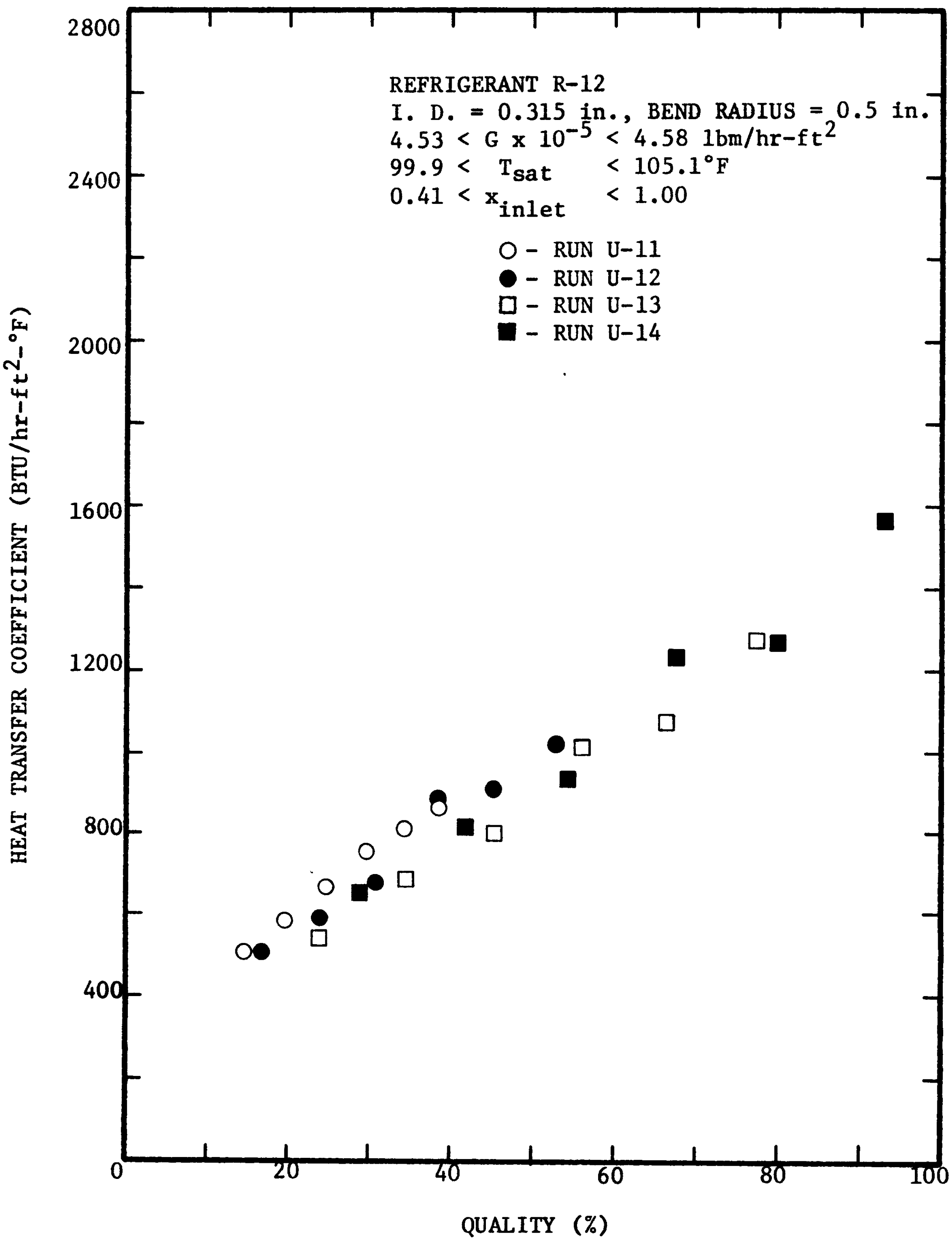

FIGURE 14 DOWNSTREAM HEAT TRANSFER COEFFICIENT vs. QUALITY

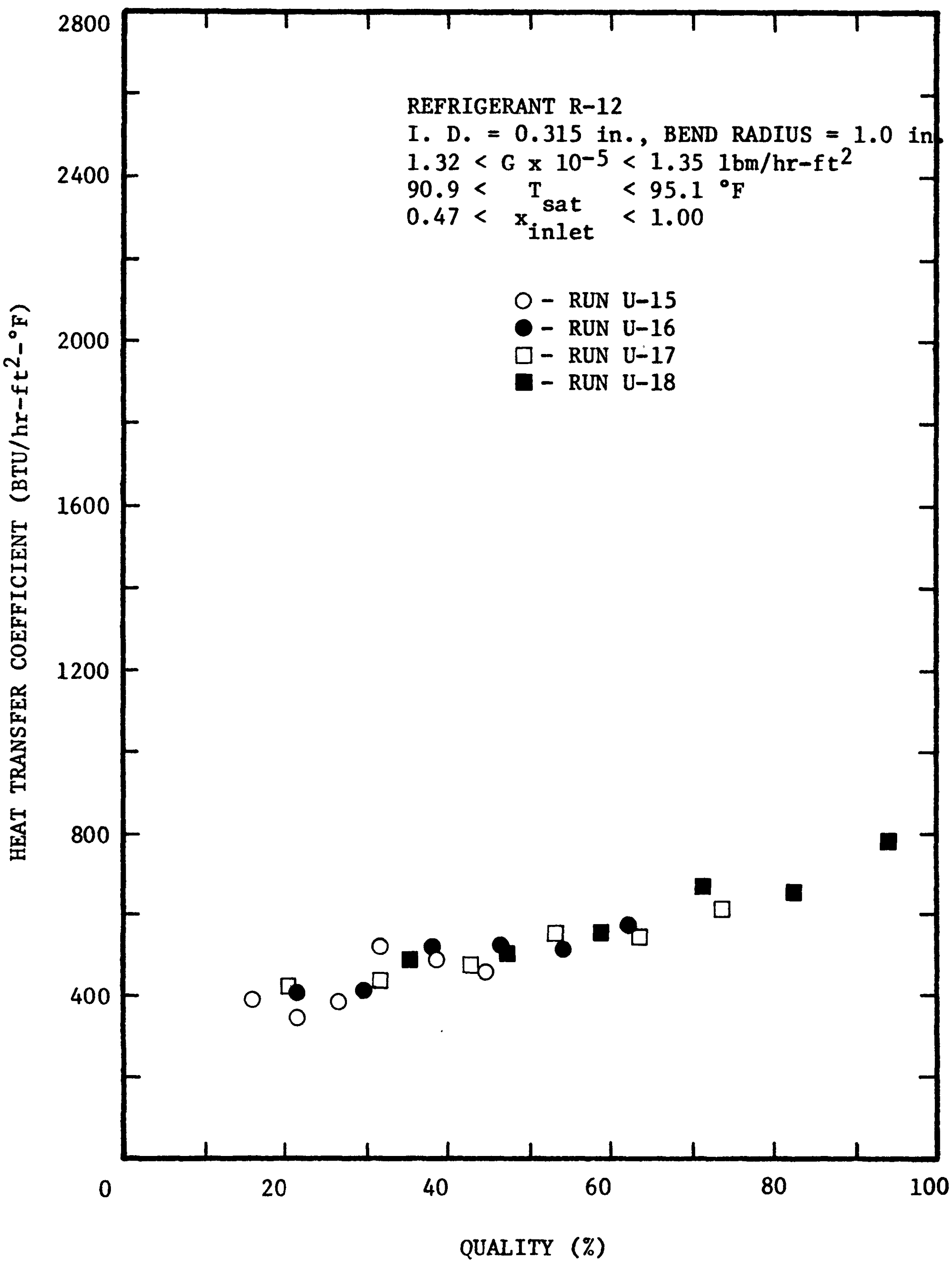

FIGURE 15 DOWNSTREAM HEAT TRANSFER COEFFICIENT vs. QUALITY

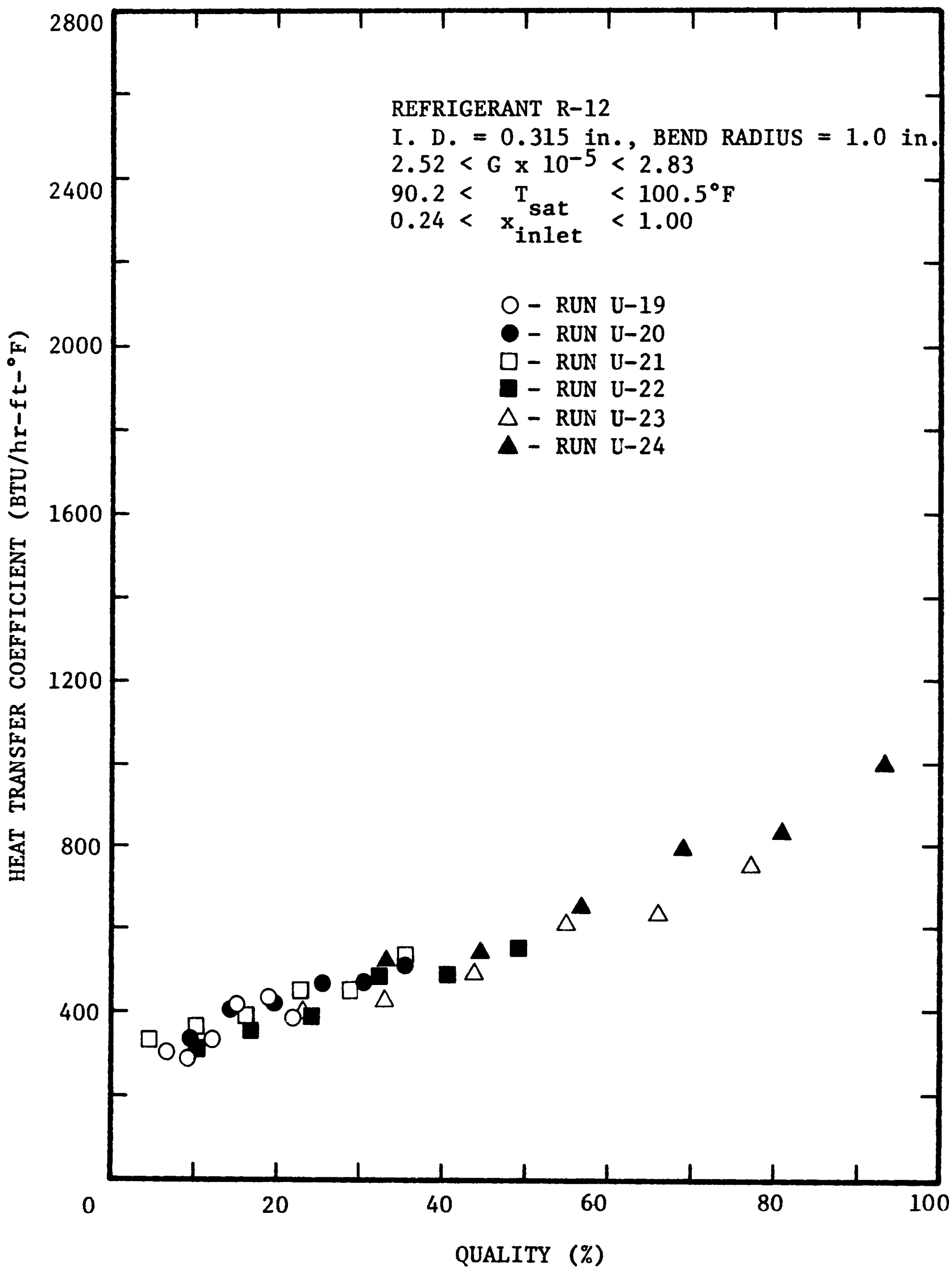

FIGURE 16 DOWNSTREAM HEAT TRANSFER COEFFICIENT vs. QUALITY

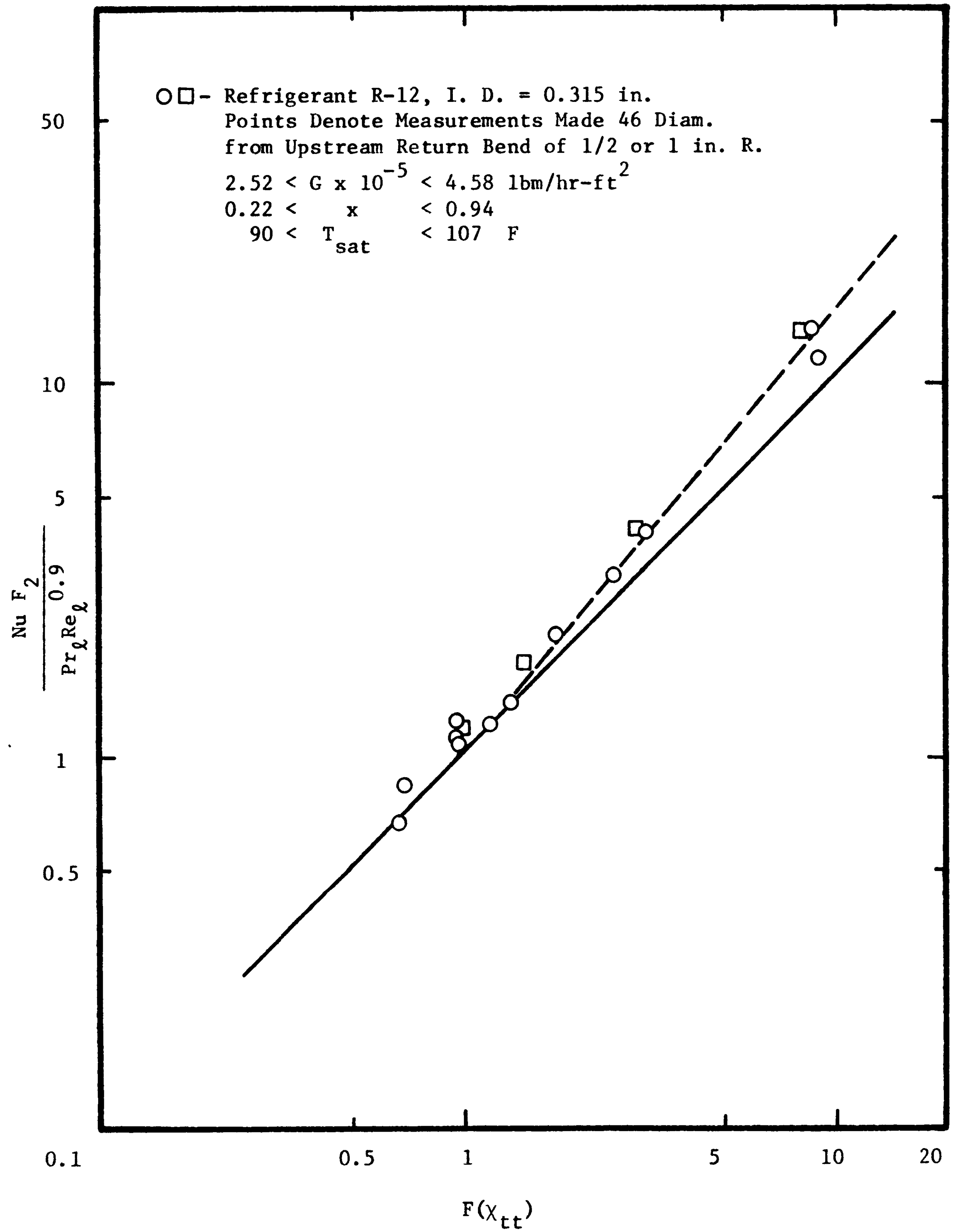

FIGURE 17 COMPARISON OF HEAT TRANSFER DATA WITH STRAIGHT TUBE ANALYSIS OF TRAVISS ET. AL.

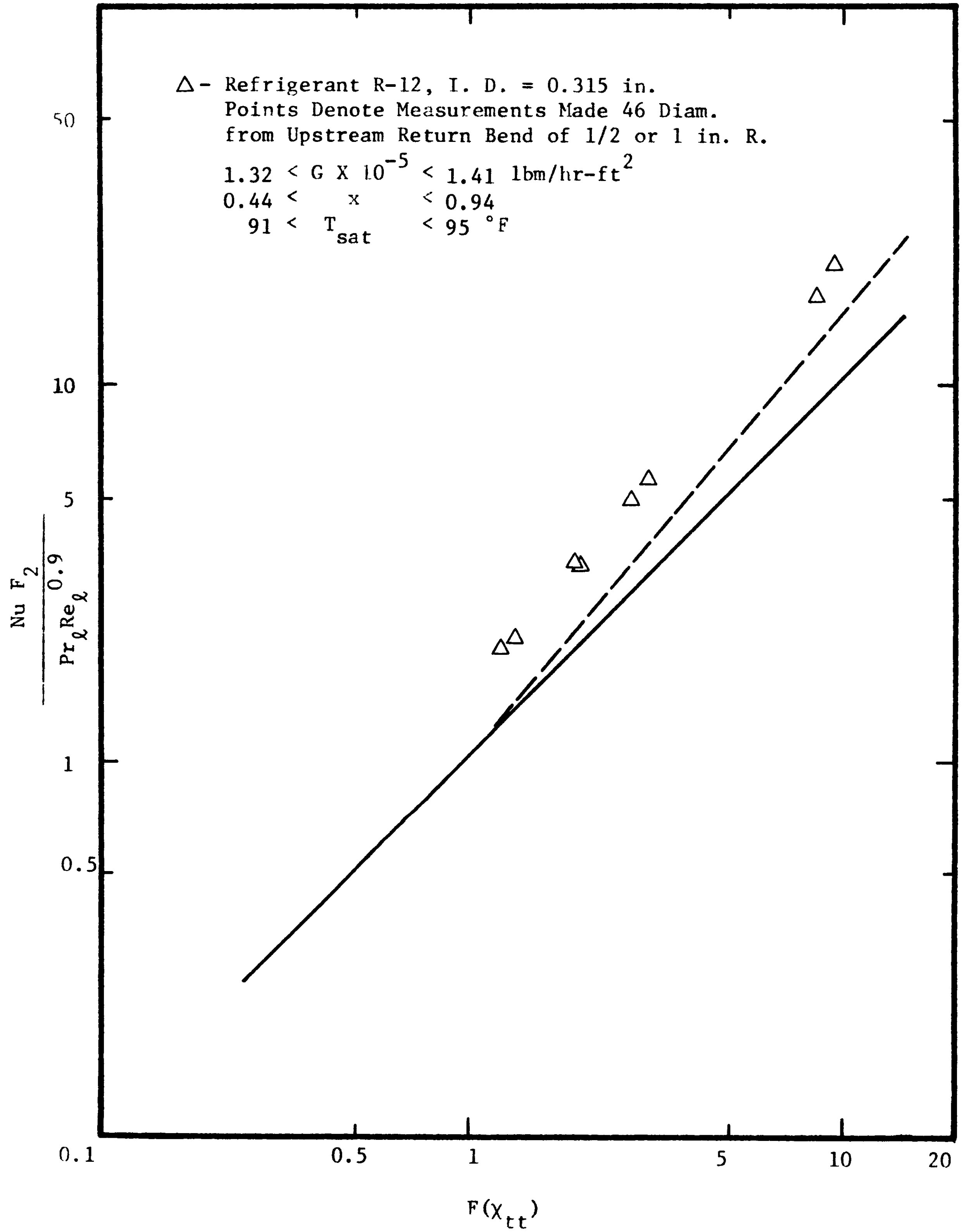

FIGURE 18 COMPARISON OF HEAT TRANSFER DATA
WITH STRAIGHT TUBE ANALYSIS OF TRAVISS ET. AL

APPENDIX 1

Data Reduction Computer Program

```
// JOB T  1130                                                  TRAVISS

LOG DRIVE   CART SPEC   CART AVAIL  PHY DRIVE
  0000        1130         1130        0000
                           1133        0001
                           1131        0002

V2 M09   ACTUAL  8K  CONFIG  8K

// FOR
*IOCS (CARD,1403 PRINTER)
* LIST SOURCE PROGRAM
      REAL NU,KL
      DIMENSION TV(6),TW(6),DTW(6),DP(6),GA(6),TWI(6),Q(6),WTD(6),FC(6),
     1H(6),X(6),XTT(6),FTT(6),ST(6)
      READ (2,21) N
21    FORMAT (I6)
      DO 7 I=1,N
      READ (2,22) PCWI,TIF,TEW,ACWC,TFC,PCT,TSAT,F12,AW,WAT,PW
22    FORMAT (11F7.0)
      READ (2,23) (TV(J),J=1,6)
      READ (2,23) (TW(J),J=1,6)
      READ (2,23) (DTW(J),J=1,6)
      READ (2,23) (DP(J),J=1,6)
23    FORMAT (6F7.0)
      A=TEW
      DO 4 K=1,6
4     A=A+DTW(K)
      GW=3.08*WAT*SQRT((500.69-(63.0-.01*A))*(63.0-.01*A))
      GAW=3.08*AW*SQRT((500.69-(63.0-.01*ACWC))*(63.0-.01*ACWC))
      GPW=3.08*PW*SQRT((500.69-(63.-.01*PCWI))*(63.-.01*PCWI))
      IF (TSAT-110) 10,10,11
10    RC=.04267*TSAT-.9936
```

```
      GC TO 12
11    RC=.06233*TSAT-3.156
12    GF=3.08*F12*SQRT((500.69-RC)*RO)
      G=(GF/.00054118)
      WSHB=GW*(A-TEW)+GAW*(ACWC-TEW)+GPW*PCT
      FSHB=GF*(72.8+.0766*TSAT-.2466*TFC)
      PEHB=(WSHB-FSHB)/WSHB
      HM=0
      QT=0
      DC 6 J=1,6
      FC(J)=DP(J)*29.16
      Q(J)=GW*DTW(J)*.998
      QA(J)=Q(J)/0.1984
      TWI(J)=TW(J)+Q(J)*.000052517
      WTD(J)=TV(J)-TWI(J)
      H(J)=QA(J)/WTD(J)
      HM=HM+H(J)/6.
      XO=(72.8+.0766*TSAT-.2466*TIF-GPW*PCT/GF)/(72.8-.17*TIF)
      IF (J-1) 13,13,14
13    X(J)=(.2466*(TIF-TV(J))+XO*(72.8-.17*TIF)-Q(J)/(2.*GF))/(72.8
     1-.17*TV(J))
      GC TO 8
14    KT=J-1
      QT=QT+Q(KT)
      X(J)=(.2466*(TIF-TV(J))+XO*(72.8-.17*TIF)-(QT+Q(J)/2.)/GF)/(72.8
     1-.17*TV(J))
C     NCN-DIMENSIONAL DATA REDUCTION
8     D=0.0262
      UL=0.7264-((0.1367*TV(J))/100.)
      UV=0.02768+((0.3583*TV(J))/10000.)
      KL=0.0447-((0.4607*TV(J))/10000.)
      RCL=93.156-(.1447*TV(J))
      CL=0.21135+((0.2835*TV(J))/1000.)
      IF(TSAT-110) 50,50,60
```

```
50     RCV=(.04267*TV(J))-.9936
       GO TO 70
60     RCV=(.06233*TV(J))-3.156
70     RU=UL/UV
       RRO=RCV/RCL
       PR=UL*CL/KL
       NU=H(J)*D/KL
       RE=((1.-X(J))*G*D)/UL
       IF(RE-50.) 80,80,85
80     F2=0.707*PR*(RE**0.5)
85     IF(RE-1125.) 90,90,95
90     F2=5.*PR+5.*ALOG(1.+PR*(.09636*(RE**.585)-1.))
95     F2=5.*PR+5.*ALOG(1.+5.*PR)+2.5*ALOG(.00313*(RE**.812))
       XTT(J)=(RU**.1)*(RRO**.5)*(((1.-X(J))/X(J))**.9)
       FTT(J)=.150*(XTT(J)**(-1.)+2.85*XTT(J)**(-.476))
       ST(J)=(NU*F2)/(PR*(RE**.9))
6      CONTINUE
       WRITE (5,31)
31     FORMAT (1H1)
24     FORMAT (2X,'RUN NO.',27X,'REFRIGERANT 12',11X,'INLET QUALITY',3X,F
      16.3/)
       WRITE (5,24) XO
       WRITE (5,26) G,TEW,TSAT
26     FORMAT (2X,'FREON MASS FLUX',1X,E15.7,3X,'WTR TEMP IN',3X,F6.2,5X,
      1'FREON TEMP IN',3X,F6.2/)
       WRITE (5,27) GW,HM,PERR
27     FORMAT (2X,'WTR FLOW RATE',4X,F7.2,10X,'MEAN HT COEF',1X,F7.1,5X,'
      1HEAT BAL ERROR',2X,F6.3,//)
       WRITE (5,35)
35     FORMAT (18X,'VAPOR TEMP',3X,'OUT WALL T',4X,'DEL WTR T',5X,'P GRAD
      1')
       WRITE (5,36)
36     FORMAT (22X,'(F)',10X,'(F)',10X,'(F)',7X,'(LBF/FT3)',/)
       DO 1 L=1,6
```

```
      WRITE (5,37) TV(L),TW(L),CTW(L),FO(L)
37    FORMAT (16X,4(2X,F8.3,3X))
1     CONTINUE
      WRITE (5,38)
38    FORMAT (/,18X,'IN WALL T',4X,'DEL WALL T',3X,'HEAT FLUX',7X,'H T C
     1OEF')
      WRITE (5,39)
39    FORMAT (21X,'(F)',11X,'(F)',5X,'(BTU/HR-FT2)',2X,'(BTU/HR-FT2-F)'/
     1)
      DO 2 M=1,6
      WRITE (5,41) TWI(M),WTD(M),QA(M),H(M)
41    FORMAT (16X,2(2X,F8.3,3X),2X,F8.1,5X,F8.1)
2     CONTINUE
      WRITE (5,42)
42    FORMAT (/,20X,'QUALITY',7X,'XTT',8X,'F(XTT)',2X,'NU*F2/PR*(RE**.9)
     1'/)
      DO 3 MK=1,6
      WRITE (5,43) X(MK),XTT(MK),FTT(MK),ST(MK)
43    FORMAT (21X,F5.3,3(1X,E12.3))
3     CONTINUE
      WRITE (5,30)
30    FORMAT (1H1)
7     CONTINUE
      END

FEATURES SUPPORTED
 IOCS

CORE REQUIREMENTS FOR
 COMMON       0  VARIABLES    272  PROGRAM   1480

RELATIVE EXECUTION ADDRESS IS 0286 (HEX)

 END OF COMPILATION
```

APPENDIX 2

Data Tables

RUN NO. U-1		REFRIGERANT 12		INLET QUALITY	0.508
FREON MASS FLUX	1.4096587E 05	WTR TEMP IN	85.00	FREON TEMP IN	91.65
WTR FLOW RATE	574.49	MEAN HT COEF	451.3	HEAT BAL ERROR	-0.000

VAPOR TEMP (F)	OUT WALL T (F)	DEL WTR T (F)	P GRAD (LBF/FT3)
91.480	89.300	0.384	4.957
91.350	89.170	0.377	4.082
91.170	89.000	0.361	4.082
91.260	88.780	0.391	3.499
91.130	88.390	0.370	3.499
91.100	88.000	0.386	2.332

IN WALL T (F)	DEL WALL T (F)	HEAT FLUX (BTU/HR-FT2)	H T COEF (BTU/HR-FT2-F)
89.311	2.168	1109.7	511.7
89.181	2.168	1089.4	502.3
89.010	2.159	1043.2	483.1
88.791	2.468	1129.9	457.7
88.401	2.728	1069.2	391.8
88.011	3.088	1115.4	361.1

QUALITY	XTT	F(XTT)	NU*F2/PR*(RE**.9)
0.481	2.746E-01	1.337E 00	2.260E 00
0.431	3.283E-01	1.183E 00	2.055E 00
0.383	3.920E-01	1.050E 00	1.846E 00
0.334	4.764E-01	9.233E-01	1.639E 00
0.284	5.863E-01	8.070E-01	1.321E 00
0.235	7.391E-01	6.965E-01	1.151E 00

RUN NO. U-2 REFRIGERANT 12 INLET QUALITY 0.679

FREON MASS FLUX 1.3584425E 05 WTR TEMP IN 85.70 FREON TEMP IN 94.22

WTR FLOW RATE 620.17 MEAN HT COEF 519.8 HEAT BAL ERROR 0.044

VAPOR TEMP (F)	OUT WALL T (F)	DEL WTR T (F)	P GRAD (LBF/FT3)
93.220	89.960	0.557	4.082
93.090	89.910	0.552	4.082
92.830	89.700	0.550	3.499
92.960	89.480	0.582	2.915
92.830	89.130	0.565	2.915
92.560	88.700	0.596	2.332

IN WALL T (F)	DEL WALL T (F)	HEAT FLUX (BTU/HR-FT2)	H T COEF (BTU/HR-FT2-F)
89.978	3.241	1737.6	535.9
89.927	3.162	1722.0	544.5
89.717	3.112	1715.7	551.3
89.498	3.461	1815.6	524.5
89.148	3.681	1762.5	478.7
88.719	3.840	1859.2	484.1

QUALITY	XTT	F(XTT)	NU*F2/PR*(RE**.9)
0.638	1.557E-01	1.998E 00	3.304E 00
0.557	2.113E-01	1.605E 00	2.830E 00
0.476	2.823E-01	1.311E 00	2.489E 00
0.392	3.847E-01	1.063E 00	2.090E 00
0.308	5.369E-01	8.541E-01	1.710E 00
0.223	7.939E-01	6.660E-01	1.569E 00

RUN NO. U-3 REFRIGERANT 12 INLET QUALITY 0.824

FREON MASS FLUX 1.3676321E 05 WTR TEMP IN 84.57 FREON TEMP IN 96.38

WTR FLOW RATE 610.01 MEAN HT COEF 518.0 HEAT BAL ERROR -0.035

VAPOR TEMP (F)	OUT WALL T (F)	DEL WTR T (F)	P GRAD (LBF/FT3)
95.430	91.780	0.765	6.998
95.350	91.430	0.668	5.831
95.000	91.130	0.717	5.248
95.090	90.350	0.752	4.082
94.870	89.830	0.757	3.499
94.810	89.000	0.774	2.915

IN WALL T (F)	DEL WALL T (F)	HEAT FLUX (BTU/HR-FT2)	H T COEF (BTU/HR-FT2-F)
91.804	3.625	2347.4	647.4
91.451	3.898	2049.7	525.7
91.152	3.847	2200.1	571.8
90.374	4.715	2307.5	489.2
89.854	5.015	2322.8	463.1
89.024	5.785	2375.0	410.5

QUALITY	XTT	F(XTT)	NU*F2/PR*(RE**.9)
0.766	9.068E-02	2.994E 00	5.717E 00
0.662	1.439E-01	2.117E 00	3.408E 00
0.563	2.099E-01	1.612E 00	2.983E 00
0.456	3.092E-01	1.232E 00	2.123E 00
0.347	4.650E-01	9.380E-01	1.724E 00
0.236	7.567E-01	6.863E-01	1.339E 00

RUN NO. U-4 REFRIGERANT 12 INLET QUALITY 1.003

FREON MASS FLUX 1.3373531E 05 WTR TEMP IN 81.52 FREON TEMP IN 96.75

WTR FLOW RATE 605.00 MEAN HT COEF 536.1 HEAT BAL ERROR 0.046

VAPOR TEMP (F)	OUT WALL T (F)	DEL WTR T (F)	P GRAD (LBF/FT3)
94.650	90.350	0.969	4.665
94.520	89.960	0.824	4.665
94.130	89.780	0.882	4.082
94.260	88.520	0.950	4.082
94.040	87.650	0.960	3.499
94.360	86.650	0.974	2.915

IN WALL T (F)	DEL WALL T (F)	HEAT FLUX (BTU/HR-FT2)	H T COEF (BTU/HR-FT2-F)
90.380	4.269	2948.9	690.7
89.986	4.533	2507.7	553.1
89.807	4.322	2684.2	621.0
88.550	5.709	2891.1	506.3
87.680	6.359	2921.5	459.4
86.680	7.679	2964.2	386.0

QUALITY	XTT	F(XTT)	NU*F2/PR*(RE**.9)
0.931	2.509E-02	8.447E 00	1.731E 01
0.799	7.550E-02	3.448E 00	5.663E 00
0.675	1.355E-01	2.213E 00	4.240E 00
0.540	2.266E-01	1.528E 00	2.582E 00
0.400	3.759E-01	1.079E 00	1.874E 00
0.257	6.801E-01	7.341E-01	1.315E 00

RUN NO. U-5		REFRIGERANT 12		INLET QUALITY	0.266
FREON MASS FLUX	2.7958431E 05	WTR TEMP IN	85.57	FREON TEMP IN	98.43
WTR FLOW RATE	584.55	MEAN HT COEF	394.8	HEAT BAL ERROR	0.006

VAPOR TEMP (F)	OUT WALL T (F)	DEL WTR T (F)	P GRAD (LBF/FT3)
98.000	93.350	0.782	6.415
97.570	92.650	0.702	5.831
97.130	92.090	0.722	5.248
97.090	91.220	0.726	4.665
96.210	90.390	0.687	4.082
95.460	89.390	0.646	2.915

IN WALL T (F)	DEL WALL T (F)	HEAT FLUX (BTU/HR-FT2)	H T COEF (BTU/HR-FT2-F)
93.373	4.626	2299.4	497.0
92.671	4.898	2064.2	421.3
92.112	5.017	2123.0	423.0
91.242	5.847	2134.7	365.0
90.411	5.798	2020.1	348.3
89.409	6.050	1899.5	313.9

QUALITY	XTT	F(XTT)	NU*F2/PR*(RE**.9)
0.237	7.718E-01	6.779E-01	8.861E-01
0.187	1.004E 00	5.760E-01	7.128E-01
0.140	1.365E 00	4.784E-01	6.826E-01
0.091	2.118E 00	3.698E-01	5.618E-01
0.046	4.022E 00	2.576E-01	5.152E-01
0.004	3.485E 01	8.316E-02	4.479E-01

RUN NO. U-6 REFRIGERANT 12 INLET QUALITY 0.398

FREON MASS FLUX 2.6855368E 05 WTR TEMP IN 82.91 FREON TEMP IN 97.35

WTR FLOW RATE 538.84 MEAN HT COEF 422.8 HEAT BAL ERROR -0.065

VAPOR TEMP (F)	OUT WALL T (F)	DEL WTR T (F)	P GRAD (LBF/FT3)
97.220	92.040	1.150	9.914
97.040	91.520	1.040	6.415
96.580	91.000	1.010	5.831
96.500	89.650	1.010	4.082
95.430	86.780	0.922	2.915
94.830	85.000	0.847	1.749

IN WALL T (F)	DEL WALL T (F)	HEAT FLUX (BTU/HR-FT2)	H T COEF (BTU/HR-FT2-F)
92.072	5.147	3117.1	605.5
91.549	5.490	2818.9	513.4
91.028	5.551	2737.6	493.1
89.678	6.821	2737.6	401.3
86.806	8.623	2499.1	289.7
85.023	9.806	2295.8	234.1

QUALITY	XTT	F(XTT)	NU*F2/PR*(RE**.9)
0.355	4.584E-01	9.468E-01	1.288E 00
0.283	6.157E-01	7.820E-01	9.996E-01
0.218	8.413E-01	6.424E-01	8.920E-01
0.152	1.250E 00	5.043E-01	6.779E-01
0.093	2.048E 00	3.770E-01	4.629E-01
0.038	4.827E 00	2.331E-01	3.559E-01

RUN NO. U-7 REFRIGERANT 12 INLET QUALITY 0.482

FREON MASS FLUX 2.7620900E 05 WTR TEMP IN 79.73 FREON TEMP IN 97.83

WTR FLOW RATE 594.89 MEAN HT COEF 402.6 HEAT BAL ERROR -0.077

VAPOR TEMP (F)	OUT WALL T (F)	DEL WTR T (F)	P GRAD (LBF/FT3)
96.750	90.300	1.120	13.705
96.380	89.460	0.967	8.747
95.910	88.740	1.050	6.998
95.700	87.040	1.025	4.957
94.780	86.300	0.985	4.082
92.700	84.870	0.858	2.332

IN WALL T (F)	DEL WALL T (F)	HEAT FLUX (BTU/HR-FT2)	H T COEF (BTU/HR-FT2-F)
90.334	6.415	3351.5	522.4
89.490	6.889	2893.7	419.9
88.772	7.137	3142.0	440.2
87.071	8.628	3067.2	355.4
86.330	8.449	2947.5	348.8
84.896	7.803	2567.5	329.0

QUALITY	XTT	F(XTT)	NU*F2/PR*(RE**.9)
0.442	3.292E-01	1.181E 00	1.227E 00
0.369	4.302E-01	9.872E-01	8.902E-01
0.300	5.678E-01	8.238E-01	8.547E-01
0.228	7.929E-01	6.665E-01	6.354E-01
0.161	1.160E 00	5.275E-01	5.816E-01
0.105	1.779E 00	4.092E-01	5.202E-01

RUN NO. U-8 REFRIGERANT 12 INLET QUALITY 0.665

FREON MASS FLUX 2.8051425E 05 WTR TEMP IN 82.48 FREON TEMP IN 102.79

WTR FLOW RATE 701.47 MEAN HT COEF 490.8 HEAT BAL ERROR 0.030

VAPOR TEMP (F)	OUT WALL T (F)	DEL WTR T (F)	P GRAD (LBF/FT3)
102.250	95.390	1.370	19.828
102.000	94.610	1.240	16.912
101.740	93.610	1.200	13.413
102.040	91.390	1.230	11.080
101.220	89.480	1.180	8.164
99.910	88.390	1.140	5.248

IN WALL T (F)	DEL WALL T (F)	HEAT FLUX (BTU/HR-FT2)	H T COEF (BTU/HR-FT2-F)
95.440	6.809	4834.1	709.8
94.655	7.344	4375.4	595.7
93.654	8.085	4234.2	523.6
91.435	10.604	4340.1	409.2
89.523	11.696	4163.7	355.9
88.431	11.478	4022.5	350.4

QUALITY	XTT	F(XTT)	NU*F2/PR*(RE**.9)
0.607	1.874E-01	1.748E 00	2.203E 00
0.499	2.775E-01	1.327E 00	1.507E 00
0.399	4.000E-01	1.036E 00	1.135E 00
0.297	6.020E-01	7.934E-01	7.772E-01
0.200	9.598E-01	5.921E-01	6.065E-01
0.109	1.805E 00	4.057E-01	5.458E-01

RUN NO. U-9		REFRIGERANT 12		INLET QUALITY	0.807
FREON MASS FLUX	2.7368562E 05	WTR TEMP IN	84.04	FREON TEMP IN	107.92
WTR FLOW RATE	686.06	MEAN HT COEF	499.9	HEAT BAL ERROR	0.019

VAPOR TEMP (F)	OUT WALL T (F)	DEL WTR T (F)	P GRAD (LBF/FT3)
108.170	99.610	1.720	27.993
108.000	98.780	1.530	23.327
107.420	97.700	1.540	19.245
107.710	95.300	1.520	14.580
106.700	93.350	1.460	11.080
103.610	90.740	1.380	5.831

IN WALL T (F)	DEL WALL T (F)	HEAT FLUX (BTU/HR-FT2)	H T COEF (BTU/HR-FT2-F)
99.671	8.498	5935.8	698.4
98.835	9.164	5280.1	576.1
97.755	9.664	5314.6	549.9
95.354	12.355	5245.6	424.5
93.402	13.297	5038.5	378.9
90.789	12.820	4762.4	371.4

QUALITY	XTT	F(XTT)	NU*F2/PR*(RE**.9)
0.733	1.163E-01	2.479E 00	3.048E 00
0.595	2.037E-01	1.647E 00	1.771E 00
0.467	3.239E-01	1.194E 00	1.340E 00
0.336	5.312E-01	8.600E-01	8.601E-01
0.213	9.238E-01	6.062E-01	6.658E-01
0.106	1.897E 00	3.941E-01	5.875E-01

RUN NO. U-10 REFRIGERANT 12 INLET QUALITY 1.001

FREON MASS FLUX 2.5618762E 05 WTR TEMP IN 77.65 FREON TEMP IN 105.17

WTR FLOW RATE 579.50 MEAN HT COEF 590.5 HEAT BAL ERROR 0.011

VAPOR TEMP (F)	OUT WALL T (F)	DEL WTR T (F)	P GRAD (LBF/FT3)
104.650	98.090	1.590	25.077
104.390	96.390	1.910	23.327
103.570	95.260	1.980	18.662
103.870	92.960	2.020	12.830
103.170	90.480	1.930	9.331
101.830	89.130	1.920	5.831

IN WALL T (F)	DEL WALL T (F)	HEAT FLUX (BTU/HR-FT2)	H T COEF (BTU/HR-FT2-F)
98.138	6.511	4634.9	711.7
96.448	7.942	5567.7	701.0
95.320	8.249	5771.8	699.6
93.021	10.848	5888.4	542.7
90.538	12.631	5626.0	445.4
89.188	12.641	5596.9	442.7

QUALITY	XTT	F(XTT)	NU*F2/PR*(RE**.9)
0.940	2.357E-02	8.905E 00	1.156E 01
0.808	7.726E-02	3.387E 00	4.279E 00
0.662	1.526E-01	2.028E 00	2.660E 00
0.510	2.702E-01	1.351E 00	1.508E 00
0.363	4.625E-01	9.412E-01	9.921E-01
0.223	8.499E-01	6.383E-01	8.345E-01

RUN NO. V-11		REFRIGERANT 12		INLET QUALITY	0.413
FREON MASS FLUX	4.5765418E 05	WTR TEMP IN	88.35	FREON TEMP IN	103.43
WTR FLOW RATE	711.43	MEAN HT COEF	703.4	HEAT BAL ERROR	0.014

VAPOR TEMP (F)	OUT WALL T (F)	DEL WTR T (F)	P GRAD (LBF/FT3)
101.870	97.910	0.952	35.575
101.570	97.480	0.931	30.909
101.390	97.040	0.913	27.993
101.570	96.250	0.988	23.619
101.130	95.300	0.957	20.411
101.070	94.350	0.960	14.580

IN WALL T (F)	DEL WALL T (F)	HEAT FLUX (BTU/HR-FT2)	H T COEF (BTU/HR-FT2-F)
97.945	3.924	3406.8	868.1
97.514	4.055	3331.7	821.5
97.074	4.315	3267.3	757.0
96.286	5.283	3535.7	669.2
95.335	5.794	3424.7	591.0
94.385	6.684	3435.5	513.9

QUALITY	XTT	F(XTT)	NU*F2/PR*(RE**.9)
0.388	4.164E-01	1.008E 00	1.227E 00
0.341	5.001E-01	8.944E-01	1.090E 00
0.294	6.072E-01	7.891E-01	9.478E-01
0.244	7.635E-01	6.825E-01	7.909E-01
0.196	9.822E-01	5.838E-01	6.629E-01
0.146	1.343E 00	4.831E-01	5.482E-01

RUN NO. U-12		REFRIGERANT 12		INLET QUALITY	0.573
FREON MASS FLUX	4.5320850E 05	WTR TEMP IN	81.04	FREON TEMP IN	101.87
WTR FLOW RATE	767.59	MEAN HT COEF	764.7	HEAT BAL ERROR	-0.018

VAPOR TEMP (F)	OUT WALL T (F)	DEL WTR T (F)	P GRAD (LBF/FT3)
101.000	95.610	1.410	47.239
100.520	94.830	1.330	40.823
99.870	94.040	1.320	34.991
99.910	92.390	1.310	29.160
99.170	90.570	1.310	23.327
99.060	89.220	1.280	14.580

IN WALL T (F)	DEL WALL T (F)	HEAT FLUX (BTU/HR-FT2)	H T COEF (BTU/HR-FT2-F)
95.666	5.333	5444.2	1020.8
94.883	5.636	5135.3	911.0
94.093	5.776	5096.7	882.2
92.442	7.467	5058.1	677.3
90.622	8.547	5058.1	591.7
89.271	9.788	4942.3	504.9

QUALITY	XTT	F(XTT)	NU*F2/PR*(RE**.9)
0.530	2.464E-01	1.441E 00	1.820E 00
0.455	3.224E-01	1.197E 00	1.433E 00
0.383	4.192E-01	1.004E 00	1.249E 00
0.309	5.626E-01	8.287E-01	8.723E-01
0.239	7.710E-01	6.783E-01	7.022E-01
0.167	1.152E 00	5.296E-01	5.552E-01

RUN NO. U-13		REFRIGERANT 12		INLET QUALITY	0.833
FREON MASS FLUX	4.5747981E 05	WTR TEMP IN	79.05	FREON TEMP IN	107.67
WTR FLOW RATE	772.59	MEAN HT COEF	896.5	HEAT BAL ERROR	-0.027

VAPOR TEMP (F)	OUT WALL T (F)	DEL WTR T (F)	P GRAD (LBF/FT3)
105.250	98.910	2.040	65.901
104.700	97.780	1.890	56.570
103.910	96.620	1.890	46.072
103.910	94.350	1.950	35.575
103.040	92.130	1.900	27.993
103.360	90.260	1.810	17.495

IN WALL T (F)	DEL WALL T (F)	HEAT FLUX (BTU/HR-FT2)	H T COEF (BTU/HR-FT2-F)
98.992	6.257	7928.1	1267.0
97.856	6.843	7345.2	1073.3
96.696	7.213	7345.2	1018.2
94.428	9.481	7578.3	799.3
92.206	10.833	7384.0	681.6
90.333	13.026	7034.2	539.9

QUALITY	XTT	F(XTT)	NU*F2/PR*(RE**.9)
0.775	9.305E-02	2.935E 00	4.154E 00
0.665	1.523E-01	2.031E 00	2.516E 00
0.560	2.260E-01	1.531E 00	1.898E 00
0.451	3.344E-01	1.168E 00	1.236E 00
0.346	4.954E-01	8.999E-01	9.093E-01
0.240	7.887E-01	6.688E-01	6.345E-01

RUN NO. U-14 | REFRIGERANT 12 | INLET QUALITY 1.003

FREON MASS FLUX 4.5277068E 05 | WTR TEMP IN 75.39 | FREON TEMP IN 107.71

WTR FLOW RATE 793.02 | MEAN HT COEF 1074.9 | HEAT BAL ERROR 0.030

VAPOR TEMP (F)	OUT WALL T (F)	DEL WTR T (F)	P GRAD (LBF/FT3)
106.570	100.520	2.330	69.983
105.960	99.040	2.160	65.026
105.080	97.910	2.180	60.069
104.960	95.430	2.210	48.405
104.000	92.830	2.260	35.575
104.030	90.570	2.180	22.453

IN WALL T (F)	DEL WALL T (F)	HEAT FLUX (BTU/HR-FT2)	H T COEF (BTU/HR-FT2-F)
100.616	5.953	9294.6	1561.2
99.129	6.830	8616.5	1261.5
98.000	7.079	8696.2	1228.3
95.521	9.438	8815.9	934.0
92.923	11.076	9015.4	813.9
90.660	13.369	8696.2	650.4

QUALITY	XTT	F(XTT)	NU*F2/PR*(RE**.9)
0.932	2.682E-02	7.984E 00	1.421E 01
0.801	8.119E-02	3.259E 00	4.627E 00
0.675	1.464E-01	2.091E 00	2.982E 00
0.546	2.390E-01	1.472E 00	1.711E 00
0.418	3.780E-01	1.075E 00	1.208E 00
0.288	6.342E-01	7.674E-01	8.143E-01

RUN NO. U-15		REFRIGERANT 12		INLET QUALITY	0.468
FREON MASS FLUX	1.3342109E 05	WTR TEMP IN	84.43	FREON TEMP IN	92.83
WTR FLOW RATE	493.14	MEAN HT COEF	439.8	HEAT BAL ERROR	-0.008

VAPOR TEMP (F)	OUT WALL T (F)	DEL WTR T (F)	P GRAD (LBF/FT3)
91.000	88.650	0.440	4.665
90.960	88.520	0.489	3.499
90.830	88.350	0.533	2.915
91.000	88.090	0.450	2.332
90.830	87.610	0.458	1.749
90.480	87.300	0.507	1.166

IN WALL T (F)	DEL WALL T (F)	HEAT FLUX (BTU/HR-FT2)	H T COEF (BTU/HR-FT2-F)
88.661	2.338	1091.4	466.7
88.532	2.427	1213.0	499.7
88.363	2.466	1322.1	536.1
88.101	2.898	1116.2	385.1
87.621	3.208	1136.1	354.1
87.313	3.166	1257.6	397.1

QUALITY	XTT	F(XTT)	NU*F2/PR*(RE**.9)
0.442	3.146E-01	1.217E 00	2.033E 00
0.387	3.859E-01	1.061E 00	2.011E 00
0.327	4.885E-01	9.082E-01	1.993E 00
0.268	6.310E-01	7.699E-01	1.334E 00
0.214	8.196E-01	6.529E-01	1.156E 00
0.158	1.141E 00	5.328E-01	1.224E 00

RUN NO. U-16 | REFRIGERANT 12 | INLET QUALITY 0.662

FREON MASS FLUX 1.3618856E 05 | WTR TEMP IN 83.64 | FREON TEMP IN 93.43

WTR FLOW RATE 498.21 | MEAN HT COFF 497.2 | HEAT BAL ERROR 0.000

VAPOR TEMP (F)	OUT WALL T (F)	DEL WTR T (F)	P GRAD (LBF/FT3)
92.610	89.610	0.687	5.248
92.520	89.390	0.644	4.082
92.260	89.090	0.674	3.499
92.090	88.570	0.731	2.915
92.260	87.910	0.714	2.332
91.570	87.170	0.726	1.749

IN WALL T (F)	DEL WALL T (F)	HEAT FLUX (BTU/HR-FT2)	H T COEF (BTU/HR-FT2-F)
89.627	2.982	1721.7	577.3
89.406	3.113	1613.9	518.4
89.107	3.152	1689.1	535.8
88.589	3.500	1831.9	523.2
87.928	4.331	1789.3	413.1
87.188	4.381	1819.4	415.3

QUALITY	XTT	F(XTT)	NU*F2/PR*(RE**.9)
0.621	1.658E-01	1.909E 00	3.416E 00
0.542	2.216E-01	1.552E 00	2.618E 00
0.465	2.922E-01	1.281E 00	2.374E 00
0.383	3.956E-01	1.043E 00	2.055E 00
0.297	5.598E-01	8.314E-01	1.454E 00
0.214	8.242E-01	6.506E-01	1.332E 00

RUN NO. U-17 REFRIGERANT 12 INLET QUALITY 0.790

FREON MASS FLUX 1.3497765E 05 WTR TEMP IN 83.26 FREON TEMP IN 96.88

WTR FLOW RATE 498.18 MEAN HT COEF 510.4 HEAT BAL ERROR 0.049

VAPOR TEMP (F)	OUT WALL T (F)	DEL WTR T (F)	P GRAD (LBF/FT3)
94.780	91.220	0.874	6.415
94.780	91.000	0.821	5.248
94.610	90.610	0.869	4.665
94.700	89.870	0.909	3.499
94.570	89.220	0.934	2.915
93.910	88.300	0.969	1.749

IN WALL T (F)	DEL WALL T (F)	HEAT FLUX (BTU/HR-FT2)	H T COEF (BTU/HR-FT2-F)
91.242	3.537	2190.2	619.2
91.021	3.758	2057.4	547.3
90.632	3.977	2177.7	547.5
89.893	4.806	2277.9	473.9
89.244	5.325	2340.6	439.4
88.325	5.584	2428.3	434.8

QUALITY	XTT	F(XTT)	NU*F2/PR*(RE**.9)
0.738	1.032E-01	2.711E 00	5.031E 00
0.637	1.587E-01	1.971E 00	3.375E 00
0.536	2.309E-01	1.508E 00	2.747E 00
0.429	3.402E-01	1.154E 00	1.997E 00
0.318	5.204E-01	8.716E-01	1.597E 00
0.207	8.751E-01	6.269E-01	1.391E 00

RUN NO. U-18		REFRIGERANT 12		INLET QUALITY	0.999
FREON MASS FLUX	1.3217937E 05	WTR TEMP IN	84.35	FREON TEMP IN	95.04
WTR FLOW RATE	579.49	MEAN HT COEF	609.5	HEAT BAL ERROR	0.084

VAPOR TEMP (F)	OUT WALL T (F)	DEL WTR T (F)	P GRAD (LBF/FT3)
95.350	92.170	0.835	6.415
95.260	91.830	0.765	5.831
94.960	91.430	0.805	5.831
95.220	90.780	0.848	5.248
95.090	90.170	0.857	4.665
94.430	89.350	0.852	3.499

IN WALL T (F)	DEL WALL T (F)	HEAT FLUX (BTU/HR-FT2)	H T COEF (BTU/HR-FT2-F)
92.195	3.154	2434.0	771.5
91.853	3.406	2229.9	654.5
91.454	3.505	2346.5	669.3
90.805	4.414	2471.9	559.9
90.196	4.893	2498.1	510.4
89.375	5.054	2483.5	491.3

QUALITY	XTT	F(XTT)	NU*F2/PR*(RE**.9)
0.939	2.225E-02	9.356E 00	2.175E 01
0.825	6.513E-02	3.871E 00	7.595E 00
0.714	1.155E-01	2.492E 00	5.134E 00
0.595	1.863E-01	1.755E 00	3.209E 00
0.474	2.894E-01	1.289E 00	2.346E 00
0.354	4.503E-01	9.580E-01	1.901E 00

RUN NO. U-19 REFRIGERANT 12 INLET QUALITY 0.240

FREON MASS FLUX 2.8283750E 05 WTR TEMP IN 80.22 FREON TEMP IN 91.04

WTR FLOW RATE 498.35 MEAN HT COEF 364.6 HEAT BAL ERROR -0.010

VAPOR TEMP (F)	OUT WALL T (F)	DEL WTR T (F)	P GRAD (LBF/FT3)
90.830	87.300	0.550	6.706
90.700	87.130	0.630	5.540
90.350	86.480	0.640	5.540
90.260	85.960	0.580	3.207
89.960	85.350	0.530	2.624
88.960	84.610	0.530	0.874

IN WALL T (F)	DEL WALL T (F)	HEAT FLUX (BTU/HR-FT2)	H T COEF (BTU/HR-FT2-F)
87.314	3.515	1378.7	392.1
87.146	3.553	1579.3	444.4
86.496	3.853	1604.3	416.3
85.975	4.284	1453.9	339.3
85.363	4.596	1328.6	289.0
84.623	4.336	1328.6	306.4

QUALITY	XTT	F(XTT)	NU*F2/PR*(RE**.9)
0.223	7.840E-01	6.712E-01	6.859E-01
0.190	9.386E-01	6.003E-01	7.506E-01
0.155	1.164E 00	5.264E-01	6.789E-01
0.121	1.506E 00	4.512E-01	5.351E-01
0.091	2.002E 00	3.820E-01	4.431E-01
0.065	2.747E 00	3.188E-01	4.591E-01

RUN NO. U-20 REFRIGERANT 12 INLET QUALITY 0.385

FREON MASS FLUX	2.8293812E 05	WTR TEMP IN	80.96	FREON TEMP IN	93.22
WTR FLOW RATE	688.99	MEAN HT COEF	443.5	HEAT BAL ERROR	-0.013

VAPOR TEMP (F)	OUT WALL T (F)	DEL WTR T (F)	P GRAD (LBF/FT3)
92.830	88.220	0.720	11.663
92.650	87.780	0.660	8.164
92.300	87.430	0.660	6.706
92.300	86.650	0.690	5.831
91.960	85.870	0.710	5.248
91.090	85.090	0.590	3.499

IN WALL T (F)	DEL WALL T (F)	HEAT FLUX (BTU/HR-FT2)	H T COEF (BTU/HR-FT2-F)
88.245	4.584	2495.3	544.3
87.803	4.846	2287.4	472.0
87.453	4.846	2287.4	472.0
86.674	5.625	2391.4	425.1
85.895	6.064	2460.7	405.7
85.111	5.978	2044.8	342.0

QUALITY	XTT	F(XTT)	NU*F2/PR*(RE**.9)
0.355	4.426E-01	9.689E-01	1.112E 00
0.302	5.505E-01	8.404E-01	9.019E-01
0.251	6.899E-01	7.275E-01	8.503E-01
0.198	9.084E-01	6.126E-01	7.228E-01
0.144	1.276E 00	4.981E-01	6.533E-01
0.097	1.905E 00	3.931E-01	5.264E-01

RUN NO. U-21 REFRIGERANT 12 INLET QUALITY 0.390

FREON MASS FLUX 2.6124593E 05 WTR TEMP IN 79.09 FREON TEMP IN 93.35

WTR FLOW RATE 701.77 MEAN HT COEF 422.1 HEAT BAL ERROR -0.004

VAPOR TEMP (F)	OUT WALL T (F)	DEL WTR T (F)	P GRAD (LBF/FT3)
92.480	87.130	0.800	11.080
92.390	86.700	0.730	6.998
92.000	86.260	0.730	5.248
92.000	85.300	0.750	4.082
91.390	84.260	0.730	2.915
90.300	83.350	0.660	1.749

IN WALL T (F)	DEL WALL T (F)	HEAT FLUX (BTU/HR-FT2)	H T COEF (BTU/HR-FT2-F)
87.159	5.320	2824.0	530.7
86.726	5.663	2576.9	455.0
86.286	5.713	2576.9	451.0
85.327	6.672	2647.5	396.7
84.286	7.103	2576.9	362.7
83.374	6.925	2329.8	336.4

QUALITY	XTT	F(XTT)	NU*F2/PR*(RE**.9)
0.355	4.417E-01	9.702E-01	1.160E 00
0.289	5.799E-01	8.127E-01	9.164E-01
0.227	7.740E-01	6.767E-01	8.467E-01
0.163	1.120E 00	5.389E-01	6.964E-01
0.101	1.820E 00	4.038E-01	5.999E-01
0.046	3.875E 00	2.630E-01	5.292E-01

RUN NO. U-22 REFRIGERANT 12 INLET QUALITY 0.539

FREON MASS FLUX 2.7804356E 05 WTR TEMP IN 81.35 FREON TEMP IN 98.83

WTR FLOW RATE 676.16 MEAN HT COEF 430.5 HEAT BAL ERROR -0.050

VAPOR TEMP (F)	OUT WALL T (F)	DEL WTR T (F)	P GRAD (LBF/FT3)
98.570	91.780	1.110	18.079
98.300	91.040	1.030	12.830
97.650	90.350	1.030	10.789
97.780	88.960	1.010	7.290
97.170	87.610	0.970	6.123
96.000	86.480	0.890	4.665

IN WALL T (F)	DEL WALL T (F)	HEAT FLUX (BTU/HR-FT2)	H T COEF (BTU/HR-FT2-F)
91.819	6.750	3775.4	559.2
91.076	7.223	3503.3	484.9
90.386	7.263	3503.3	482.3
88.995	8.784	3435.3	391.0
87.644	9.525	3299.2	346.3
86.511	9.488	3027.1	319.0

QUALITY	XTT	F(XTT)	NU*F2/PR*(RE**.9)
0.494	2.764E-01	1.331E 00	1.416E 00
0.409	3.756E-01	1.080E 00	1.078E 00
0.329	5.100E-01	8.830E-01	9.634E-01
0.247	7.324E-01	7.006E-01	7.087E-01
0.170	1.110E 00	5.416E-01	5.786E-01
0.101	1.891E 00	3.949E-01	4.985E-01

RUN NO. U-23		REFRIGERANT 12		INLET QUALITY	0.833
FREON MASS FLUX	2.5172568E 05	WTR TEMP IN	80.48	FREON TEMP IN	100.87
WTR FLOW RATE	719.37	MEAN HT COEF	545.0	HEAT BAL ERROR	-0.032

VAPOR TEMP (F)	OUT WALL T (F)	DEL WTR T (F)	P GRAD (LBF/FT3)
99.260	93.170	1.250	25.369
99.130	92.390	1.180	19.537
98.780	91.780	1.160	16.038
99.000	90.220	1.180	11.372
98.700	88.650	1.160	9.039
97.830	87.300	1.080	5.248

IN WALL T (F)	DEL WALL T (F)	HEAT FLUX (BTU/HR-FT2)	H T COEF (BTU/HR-FT2-F)
93.217	6.042	4523.3	748.5
92.434	6.695	4270.0	637.7
91.823	6.956	4197.6	603.4
90.264	8.735	4270.0	488.8
88.693	10.006	4197.6	419.5
87.340	10.489	3908.1	372.5

QUALITY	XTT	F(XTT)	NU*F2/PR*(RE**.9)
0.775	8.920E-02	3.032E 00	4.078E 00
0.661	1.489E-01	2.065E 00	2.459E 00
0.552	2.247E-01	1.537E 00	1.840E 00
0.441	3.359E-01	1.164E 00	1.237E 00
0.332	5.083E-01	8.849E-01	9.136E-01
0.229	7.993E-01	6.632E-01	7.201E-01

RUN NO. U-24 REFRIGERANT 12 INLET QUALITY 1.000

FREON MASS FLUX 2.8029593E 05 WTR TEMP IN 79.59 FREON TEMP IN 101.35

WTR FLOW RATE 721.88 MEAN HT COEF 726.7 HEAT BAL ERROR 0.024

VAPOR TEMP (F)	OUT WALL T (F)	DEL WTR T (F)	P GRAD (LBF/FT3)
101.390	95.870	1.510	29.160
101.090	94.910	1.410	23.911
100.520	94.130	1.390	22.161
100.610	92.430	1.470	18.079
100.090	90.550	1.420	16.329
99.090	89.130	1.430	11.663

IN WALL T (F)	DEL WALL T (F)	HEAT FLUX (BTU/HR-FT2)	H T COEF (BTU/HR-FT2-F)
95.927	5.462	5483.1	1003.7
94.963	6.126	5120.0	835.7
94.182	6.337	5047.4	796.4
92.485	8.124	5337.9	657.0
90.603	9.486	5156.3	543.5
89.184	9.905	5192.6	524.2

QUALITY	XTT	F(XTT)	NU*F2/PR*(RE**.9)
0.935	2.492E-02	8.496E 00	1.416E 01
0.811	7.423E-02	3.494E 00	4.805E 00
0.692	1.319E-01	2.257E 00	3.044E 00
0.570	2.125E-01	1.599E 00	1.894E 00
0.449	3.289E-01	1.181E 00	1.270E 00
0.331	5.115E-01	8.814E-01	1.041E 00

APPENDIX 3

Description of the Forced-Convection Condensation Parameters Used in Figures 17 and 18

The correlating parameters used in Figs. 17 and 18 were analytically determined by Traviss, Baron, and Rohsenow [6] for high mass velocity condensation inside a straight tube with a straight inlet section. The von Karman universal velocity profile was applied to the condensate flow, wall shear stress was calculated using the Lockhart-Martinelli correlation, and heat transfer coefficients were determined from the momentum and heat transfer analogy.

The analysis was then compared to experimental data. These data were determined from heat transfer measurements of refrigerants R-12 and R-22 condensing in a copper tube, 14.5 ft. long and 0.315 in. inside diameter. The analysis, represented by the lines, and the data, represented by the points, are depicted by Fig. A3-1. The correlating parameters were evaluated from the following equations:

$$Nu = \frac{(q/A)\ D}{(T_{sat} - T_w)\ k_\ell} \tag{1}$$

$$Re_\ell = \frac{G\ (1-x)\ D}{\mu_\ell} \tag{2}$$

$$\chi_{tt} \equiv \left(\frac{1-x}{x}\right)^{0.9} \left(\frac{\rho_v}{\rho_\ell}\right)^{0.5} \left(\frac{\mu_\ell}{\mu_v}\right)^{0.1} \tag{3}$$

$$F(\chi_{tt}) \equiv 0.15\ (\chi_{tt}^{\ -1} + 2.85\ \chi_{tt}^{\ -0.476}) \tag{4}$$

$$F_2 \equiv 0.707\ Pr_\ell Re_\ell^{\ 1/2} \qquad Re_\ell < 50 \tag{5}$$

$$F_2 \equiv 5\ Pr_\ell + 5\ \ln[1 + Pr_\ell(0.09363\ Re_\ell^{0.585} - 1)] \qquad (6)$$

$$50 < Re_\ell < 1125$$

$$F_2 \equiv 5\ Pr_\ell + 5\ \ln[1 + 5\ Pr_\ell] + 2.5\ \ln[0.00313\ Re_\ell^{0.812}] \qquad (7)$$

$$Re_\ell > 1125$$

The solid line in Fig. A3-1 may be expressed as:

$$\frac{Nu\ F_2}{Pr_\ell Re_\ell^{0.9}} = F(\chi_{tt}) \qquad 0.1 < F(\chi_{tt}) < 1 \quad (8)$$

and the dotted line as:

$$\frac{Nu\ F_2}{Pr_\ell Re_\ell^{0.9}} = [F(\chi_{tt})]^{1.15} \qquad 1 < F(\chi_{tt}) < 20 \quad (9)$$

In order to express the experimental data in terms of the correlating parameters, the data was reduced in the following manner. Initially, the average quality for a test section zone was determined from a heat balance, and the refrigerant properties were evaluated at the saturation temperature. Using the quality (x), properties (μ, ρ), mass flux (G), and diameter (D), the parameters Re_ℓ, χ_{tt}, and F_2 were calculated. The average Nusselt number for a zone was then determined from the measured heat transfer coefficient. Finally, the correlating parameters $F(\chi_{tt})$ and $Nu\ F_2/Pr_\ell Re_\ell^{0.9}$ were evaluated and plotted. All of these computations were executed as part of the overall data reduction computer program. The results are given in Appendix 2.

It should be noted that at very high qualities ($0.95 < x < 1$) or low qualities ($x < 0.10$) the variables Re_ℓ and χ_{tt} change very rapidly with relatively small quality changes. At high qualities some error may result if the quality increment is too large due to the incremental nature of the equations of F_2, eqs. (5), (6), and (7). At low qualities, a small uncertainty in the measured quality causes a larger uncertainty in χ_{tt}, and, consequently, more data scatter.

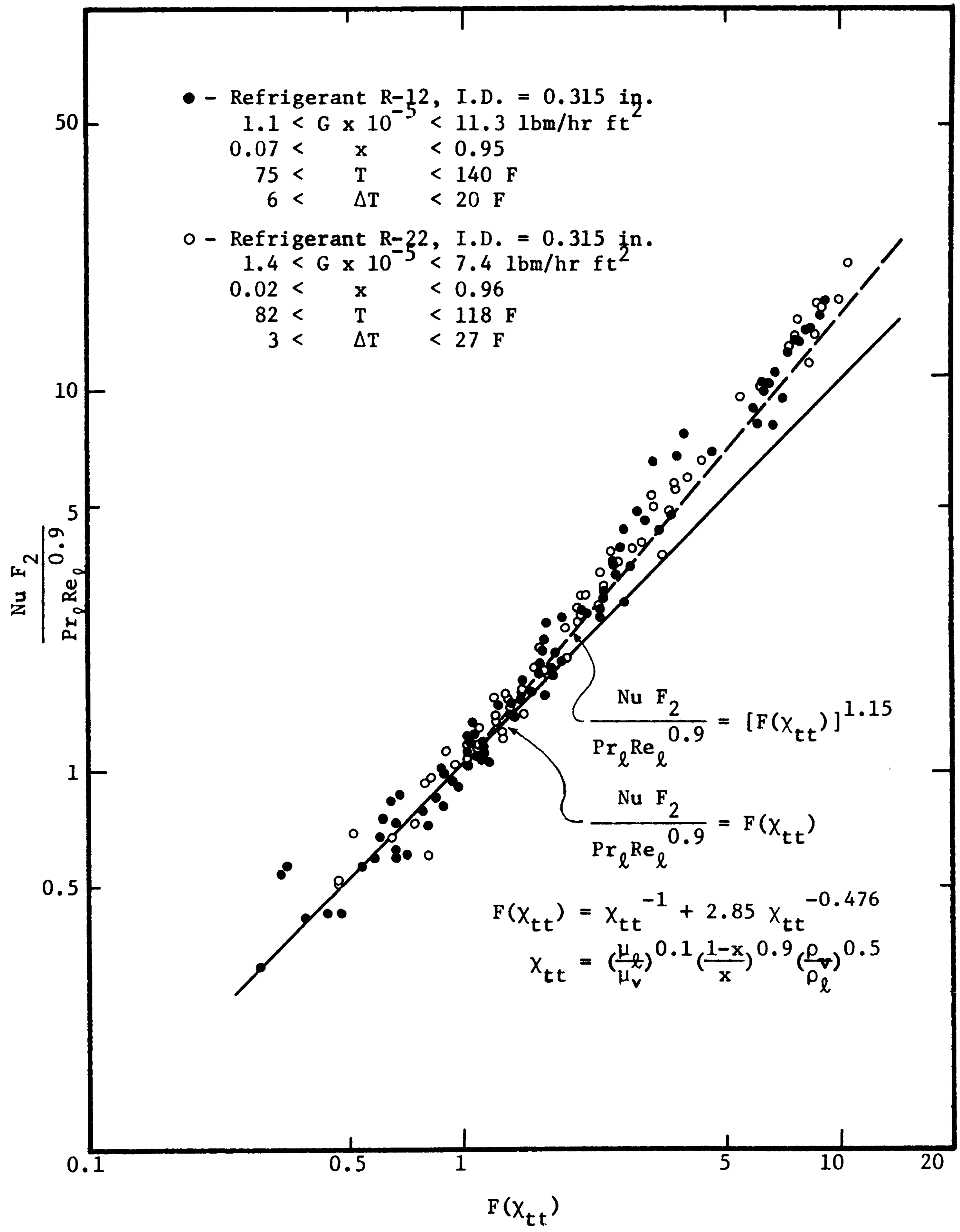

FIGURE A3-1 FORCED-CONVECTION CONDENSATION ANALYSIS AND EXPERIMENTAL DATA FROM REFERENCE [6]